

AD-A161 012

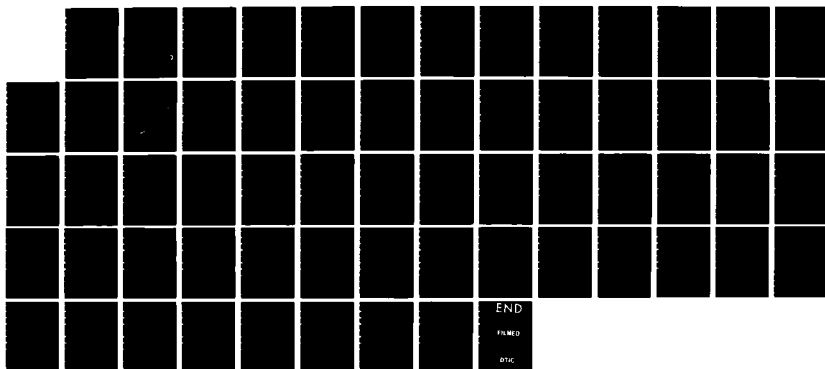
BASIC STUDIES OF GASES FOR FAST SWITCHES(U) OAK RIDGE
NATIONAL LAB TN L G CHRISTOPHOROU ET AL NOV 85
N00014-82-F-0123

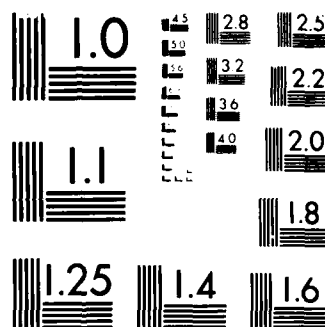
1/1

UNCLASSIFIED

F/G 9/1

NL





MICROCOPY RESOLUTION TEST CHART
NATIONAL BUREAU OF STANDARDS 1963-A

12

AD-A161 012

Interagency Agreement DOE No. 40-1246-82
Navy No. N00014-82-F-0123

Office of Naval Research
Physics Division
Arlington, Virginia 22217

BASIC STUDIES OF GASES FOR FAST SWITCHES

Annual Summary Report
October 1, 1984 to September 30, 1985

by

L. G. Christophorou and S. R. Hunter
Health and Safety Research Division

Oak Ridge National Laboratory
P. O. Box X
Oak Ridge, Tennessee 37831

November 1985

DTIC
ELECTE
NOV 07 1985
S E D

DTIC FILE COPY

Reproduction in whole or in part is permitted for any purpose of the
United States Government.

This document has been approved
for public release and sale. Its
distribution is unlimited.

85 11 07 002

UNCLASSIFIED

SECURITY CLASSIFICATION OF THIS PAGE (When Data Entered)

REPORT DOCUMENTATION PAGE		READ INSTRUCTIONS BEFORE COMPLETING FORM
1. REPORT NUMBER	2. GOVT ACCESSION NO.	3. RECIPIENT'S CATALOG NUMBER
AD-A161 012		
4. TITLE (and Subtitle) Basic Studies of Gases for Fast Switches		5. TYPE OF REPORT & PERIOD COVERED Annual Summary Report 10/1/84-9/30/85
		6. PERFORMING ORG. REPORT NUMBER
7. AUTHOR(s) L. G. Christophorou and S. R. Hunter		8. CONTRACT OR GRANT NUMBER(s) DOE No. 40-1246-82 Navy No. N00014-82-F-0123
9. PERFORMING ORGANIZATION NAME AND ADDRESS Oak Ridge National Laboratory P. O. Box X Oak Ridge, TN 37831		10. PROGRAM ELEMENT, PROJECT, TASK AREA & WORK UNIT NUMBERS
11. CONTROLLING OFFICE NAME AND ADDRESS Physics Division, Code 421 Office of Naval Research Arlington, VA 22217		12. REPORT DATE November 1985
		13. NUMBER OF PAGES
14. MONITORING AGENCY NAME & ADDRESS (if different from Controlling Office)		15. SECURITY CLASS. (of this report) UNCLASSIFIED
		15a. DECLASSIFICATION/DOWNGRADING SCHEDULE
16. DISTRIBUTION STATEMENT (of this Report) Approved for public release: distribution unlimited.		
17. DISTRIBUTION STATEMENT (of the abstract entered in Block 20, if different from Report)		
18. SUPPLEMENTARY NOTES		
19. KEY WORDS (Continue on reverse side if necessary and identify by block number) Diffuse-discharge switches; electron drift velocity; attachment rate constants; high voltage breakdown; gas mixtures, electron transport; perfluorocarbons. <i>Powering devices</i>		
20. ABSTRACT (Continue on reverse side if necessary and identify by block number) Desirable electron attachment and electron drift characteristics of gases for possible use in diffuse-discharge switches are indicated. Gas mixtures for possible use in externally sustained (e-beam) diffuse-discharge switches are suggested on the basis of electron attachment rate constants and electron drift velocities measured as a function of the density-normalized electric field E/N. Of particular promise are mixtures of Ar and C ₃ F ₈ .		

DD FORM 1473
1 JAN 73EDITION OF 1 NOV 65 IS OBSOLETE
S/N 0102-LF-014-6601

UNCLASSIFIED

SECURITY CLASSIFICATION OF THIS PAGE (When Data Entered)

BASIC STUDIES OF GASES FOR FAST SWITCHES

L. G. Christophorou and S. R. Hunter

Oak Ridge National Laboratory
Oak Ridge, Tennessee 37831

I. INTRODUCTION



A-1

This annual report contains a summary of the progress that we have made during the past year on the identification and optimization of fast gas mixtures for use in diffuse-discharge switches. Our measurements of the key transport parameters and breakdown strength characteristics of several gas mixtures which we have suggested for use in practical switching devices have recently been published¹⁻¹³ or have been submitted for publication.¹⁴⁻¹⁷

During the present contractual period, we have expanded the scope of our research program to include not only the measurement of the basic transport and rate coefficients [i.e., the electron drift velocity w , the electron attachment and ionization coefficients, η/N and α/N , respectively, the gas ionizing W values, and the high voltage breakdown field strengths $(E/N)_{lim}$] of gas mixtures of potential practical interest but also to study the behavior of these gas mixtures under more severe environmental conditions which are likely to occur in practical applications. In this connection, we have continued our studies of w , η/N , α/N , and k_a (the electron attachment rate constant) as a function of gas temperature T and have initiated new projects to study the effect of gas temperature on the $(E/N)_{lim}$ and the W value of selected gas mixtures. This information is crucial to the understanding of the mechanisms limiting the rapid recovery of the dielectric properties of the gas mixture after the switch has opened (i.e., the switch current

has decreased to zero) and the high repetition rate operation of the switch at elevated gas temperatures. We performed these studies in collaboration with a sister program funded by the Naval Surface Weapons Center (NSWC) to study the short- and long-term decomposition of these gas mixtures under varying levels of discharge current and deposited energy at elevated gas temperatures with different electrode and insulator materials.¹⁸ The modifications we have made to our experimental apparatus to allow measurements to be made at elevated gas temperatures are given in Section II, and the technical progress we have made on the identification of gas mixtures with desirable electron transport and rate coefficient properties for use in diffuse gas discharge switching applications are given in Section III.

II. TECHNIQUES

We have used experimental techniques that have been developed in this laboratory during the past ten years or so to identify gases and gas mixtures which have the desirable characteristics outlined in Refs. 1-7 and 14 when used in diffuse discharge opening switches. These measurements have allowed us to tailor gas mixtures which can optimize the characteristics required in a given switching configuration.

Measurements of w in pure gases and gas mixtures have been made in the apparatus described by Christophorou et al.¹⁹⁻²¹ This apparatus has been used to measure w in gas mixtures for use in high speed proportional counters and to study the density dependence of w in dense polar gases.²¹

We have recently used this apparatus to measure w and the electron attachment and ionization coefficients (η/N and α/N , respectively) in

gas mixtures at elevated gas temperatures. However, we have experienced severe difficulties in performing these measurements at temperatures above 500 K, as we have noticed that at higher gas temperatures the electrical insulation material used in the high voltage and signal feedthroughs loses its high impedance and becomes partially conducting. We have attempted to overcome this problem by redesigning the oven heating system to allow forced air cooling of the high voltage and signal feedthroughs. These modifications have recently been completed, and measurements at higher gas temperatures will recommence shortly.

Extensive modifications have also been made to our room temperature high voltage breakdown apparatus to allow measurements of $(E/N)_{lim}$ to be made at gas temperatures up to 600 K. These modifications included redesigning the chamber flanges and cathode support assemblies to remove any possibility of gas contamination from O-ring and vacuum grease emissions at high temperatures. We have previously observed that the electron attachment rate constant for several gases can either decrease or increase significantly with gas temperature at temperatures up to 600 K,^{11,13} and we expect that the $(E/N)_{lim}$ value for these gases will similarly be a considerable function of the gas temperature T . These findings will have important consequences for the repetitive operation of diffuse gas discharge switches at these elevated gas temperatures and the recovery of the dielectric properties of the gas after a switching impulse has occurred. Work has also commenced on modifying our W value (eV to produce an ion pair) apparatus to allow operation at elevated gas temperatures (up to 600 K).

II. TECHNICAL PROGRESS

The measurements that have been performed during this reporting period have allowed us to continue our studies on identifying attaching gas/buffer gas mixtures which have very desirable electron attaching and drift velocity characteristics for possible use in diffuse discharge opening switches. Our measurements of the electron attachment rate constants and negative ion production cross sections for several electronegative gases with the desirable electron attaching properties have now been published.^{8-11,13}

A. Basic Data

We have measured the electron attachment and ionization coefficients and electron drift velocities in O_2 , CH_4 , CF_4 , C_2F_6 , C_3F_8 , and $n-C_4F_{10}$ gases using a new method of data analysis. The pressure dependence of the electron attachment coefficient in O_2 , C_3F_8 , and $n-C_4F_{10}$ and of the electron drift velocity in C_3F_8 and $n-C_4F_{10}$ have been analyzed and explained. A paper describing this technique and the measurements we have performed in these gases has been presented at the Joint Symposium on Swarm Studies and Inelastic Electron-Molecule Collisions²² and is being prepared as an open literature publication.

High pressure electron attachment rate constant measurements ($k_a = n_w/N$) have been obtained in N_2 and Ar buffer gases for the perfluoroethers $(CF_3)_2O$ and $(CF_3)_2S$ from thermal energy (~ 0.04 eV) to ~ 4.8 eV. Both $(CF_3)_2S$ and $(CF_3)_2O$ have very desirable electron attaching properties for use in diffuse discharge switches. Knowledge of the electron energy distribution functions for N_2 and Ar buffer gases has enabled us to obtain the electron attachment cross sections (σ_a) for these electronegative gases from such measurements. Single collision negative ion

production studies have been performed for these gases which have identified the initial negative ion and neutral fragments which will be produced during the operation of the switching gas discharge. These measurements have recently been published.¹⁰ Our measurements of $k_a(\langle\epsilon\rangle)$ and the swarm unfolded attachment cross sections in the perfluoroalkanes $n\text{-C}_N\text{F}_{2N+2}$ ($N = 1-6$) have also been published.⁹ All these gases have been found to possess very desirable electron attachment properties as a function of $\langle\epsilon\rangle$ for use in diffuse gas discharge switching studies.

Measurements of the electron attachment rate constant, k_a , have been made as a function of the mean electron energy, $\langle\epsilon\rangle$, at gas temperatures up to 700 K in CCl_2F_3 and up to 750 K in C_2F_6 . A substantial increase in the rate of electron attachment with gas temperature has been observed in both of these molecules, which is interpreted as electron attachment to higher vibrational levels of the ground state of these molecules. A paper describing these measurements has been published.¹¹

Measurements of $k_a(\langle\epsilon\rangle)$ in C_3F_8 have also been performed recently as a function of gas temperature up to 750 K in argon buffer gas (over the mean electron energy range $0.76 \leq \langle\epsilon\rangle \leq 4.8$ eV). These measurements show that at $T = 300$ and 400 K, $k_a(\langle\epsilon\rangle)$ is strongly dependent on gas pressure indicating that parent negative ion formation processes are significant electron attachment processes at these temperatures. At higher gas temperatures ($T \geq 450$ K) pressure dependent attachment processes are absent indicating that electron attachment to C_3F_8 at these temperatures is purely dissociative. The overall rate of electron attachment has been found to initially decrease with increasing T up to

$T = 450$ K and significantly increase with increasing T above this gas temperature. These measurements indicate that relatively small changes in the gas kinetic energy (and hence in the vibrational populations of the attaching gas) can have a large influence on the electron attaching properties of a gas molecule which could, in turn, significantly affect the performance of repetitively operated switches operating at elevated gas temperatures using these gas mixtures. A paper describing these measurements has recently been published.¹³

Electron drift velocity measurements have been made in many gas mixtures, including CF_4/Ar , CF_4/CH_4 , $\text{C}_2\text{F}_6/\text{Ar}$, $\text{C}_2\text{F}_6/\text{CH}_4$, $\text{C}_3\text{F}_8/\text{Ar}$, $\text{C}_3\text{F}_8/\text{CH}_4$, $\text{CF}_3\text{OCF}_3/\text{Ar}$, $\text{CF}_3\text{OCF}_3/\text{CH}_4$, $\text{C}_2\text{F}_6/\text{N}_2$, $\text{CF}_4/\text{C}_2\text{F}_6$, and Ar/CH_4 over a concentration range of 0.1-100% of the attaching gas in the buffer gas. All these mixtures, except the $\text{C}_2\text{F}_6/\text{N}_2$ mixture, exhibit a pronounced negative differential conductivity region over a wide range of fractional concentrations of the attaching gas in the buffer gas, and the position of the maximum in the drift velocity is greatly affected by the concentration of the attaching gas.⁷ The ability to tailor the gas mixture to obtain the desired mobility enhancement over the appropriate E/N range is essential in order to optimize the operating conditions of the diffuse discharge in the switch. Measurements of the ratio of the transverse diffusion coefficient to the electron mobility, D_T/μ , have been made in the attaching gases CF_4 and C_2F_6 each in the buffer gases CH_4 and Ar , using the D_T/μ apparatus at the Australian National University. Preliminary data analysis has been made on the measurements in the $\text{C}_2\text{F}_6/\text{CH}_4$ gas mixtures. A paper describing these measurements has been accepted for publication.¹⁴

An extensive series of measurements of the W value (eV/ip) have been made in several binary and ternary gas mixtures containing C_2F_6 . The apparent W value of pure C_2F_6 has been found to be very dependent on the total gas pressure and applied voltage due to the large negative ion-positive ion recombination coefficient in this gas. The true W value of C_2F_6 has been found to be 34.7 eV/ion pair from an extrapolation of these measurements to infinite applied voltages. W values have also been obtained in the binary gas mixtures C_2F_6/Ar , C_2F_6/C_2H_2 , $C_2F_6/2-C_4H_8$, C_2H_2/Ar , and $2-C_4H_8/Ar$. Penning ionization processes have been found to significantly decrease the W value (i.e., to significantly increase the amount of ionization) in the latter two gas mixtures and appear to be absent in the first three mixtures. Measurements of the W value have also been made in the ternary gas mixtures $C_2F_6/Ar/2-C_4H_8$ and $C_2F_6/Ar/C_2H_2$. The measurements in the $C_2F_6/Ar/2-C_4H_8$ gas mixtures indicate that gas mixtures containing Ar and C_2F_6 and a small percentage of low ionization potential impurity (such as C_2H_2 or $2-C_4H_8$) can be tailored so as to minimize the W value of the gas mixture and hence to optimize the efficiency of electron production in an e-beam-controlled diffuse discharge switch. A paper describing these measurements and the theoretical analysis of these results has recently been published.¹²

A new set of W -value measurements has been obtained for pure CF_4 , C_2F_6 , and C_3F_8 . Surprisingly, we have found that the W values of these molecules are almost identical, even though their inelastic and ionization cross sections are considerably different. Measurements of W have also been performed in the following binary gas mixtures: CH_4/C_2F_6 , CH_4/CF_4 , Ar/CF_4 , and Ar/C_3F_8 . Some of these mixtures have been used in small-scale switching experiments, and the present measurements will be

useful in attempting to model the electron conduction properties in these experiments. We have also measured W values in the following ternary Penning ionization gas mixtures: $\text{CF}_4/\text{Ar}/\text{C}_2\text{H}_2$ and $\text{C}_3\text{F}_8/\text{Ar}/\text{C}_2\text{H}_2$. Considerable reductions in the measured W value occur (i.e., gas ionization increases) when small percentages of C_2H_2 are added to the CF_4/Ar and $\text{C}_3\text{F}_8/\text{Ar}$ gas mixtures as was previously observed for the $\text{C}_2\text{F}_6/\text{Ar}/\text{C}_2\text{H}_2$ gas mixtures.¹² Analysis of these measurements is in progress.

Measurements of the electron drift velocity and attachment and ionization coefficients have been made in $\text{C}_2\text{F}_6/\text{Ar}$ and $\text{C}_2\text{F}_6/\text{CH}_4$ gas mixtures at gas temperatures of 300 and 500 K over the concentration range of 0.1 to 100% of the C_2F_6 . These measurements are given in Figs. 1 to 5. The electron ionization coefficient in C_2F_6 is unchanged by increases in the gas temperature (Fig. 1), whereas the attachment coefficient increases significantly with T for all concentrations of C_2F_6 in either Ar (Fig. 2) or CH_4 (Fig. 3). In contrast, the electron drift velocity is hardly affected by changes in T at high E/N values near the maximum, particularly at small concentrations of the C_2F_6 (Figs. 4 and 5), but the electron mobility ($\mu_N = w/E/N$) is very dependent on T at E/N values near thermal (Figs. 6 and 7). These observations are interpreted in terms of the changes in the electron scattering processes from the higher ground state vibrational levels and increased total electron attachment cross section of C_2F_6 at elevated gas temperatures. Further measurements at 700 K are planned for the near future.

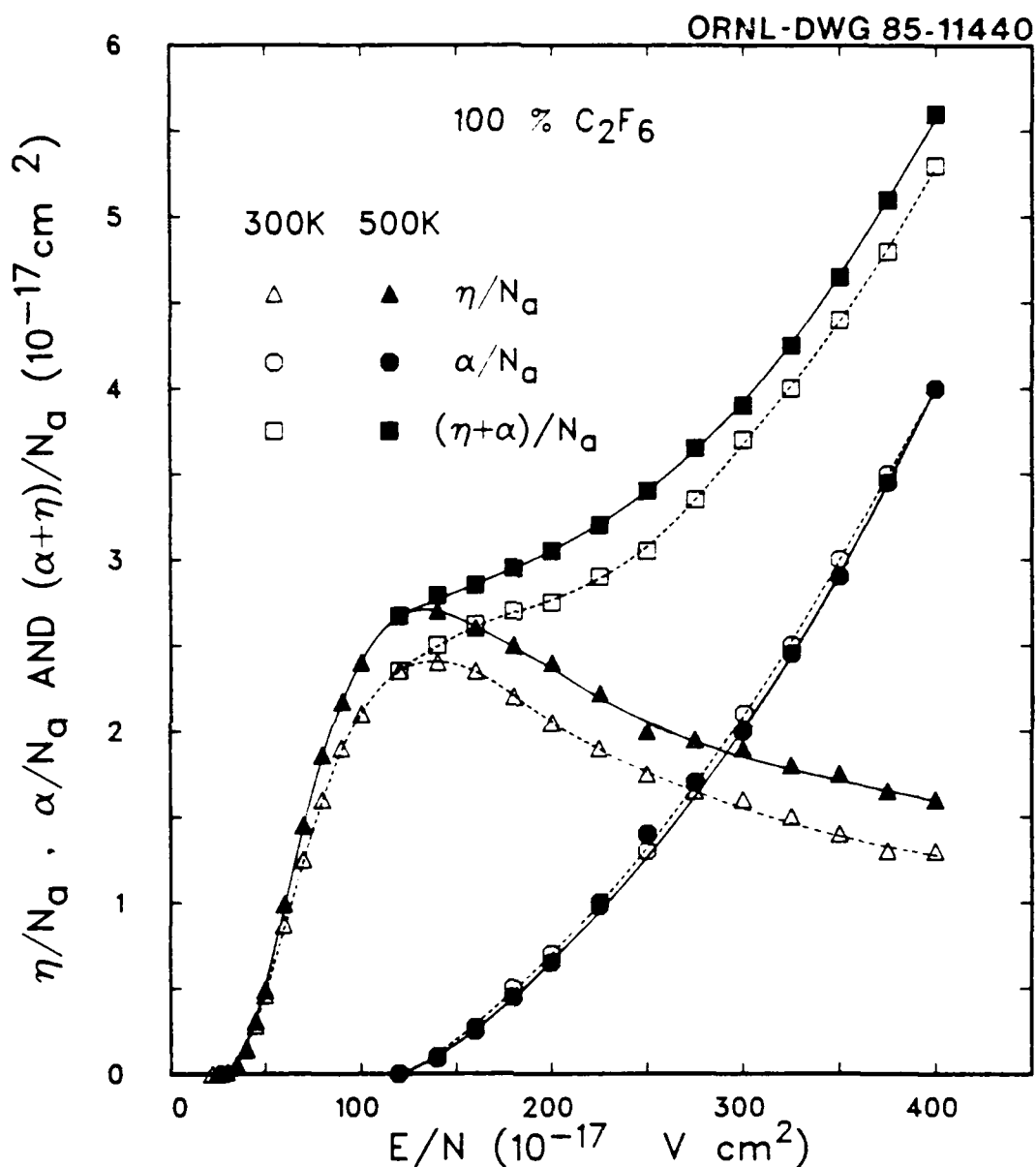


FIG. 1. Electron attachment coefficient η/N_0 , electron ionization coefficient α/N_0 , and total ion production coefficient $(\alpha+\eta)/N_0$ of pure C₂F₆ at 300 and 500 K as a function of E/N . These measurements show that the ionization coefficient is practically unchanged by increases in gas temperature, while η/N_0 increases considerably (by $\approx 25\%$) at higher E/N values.

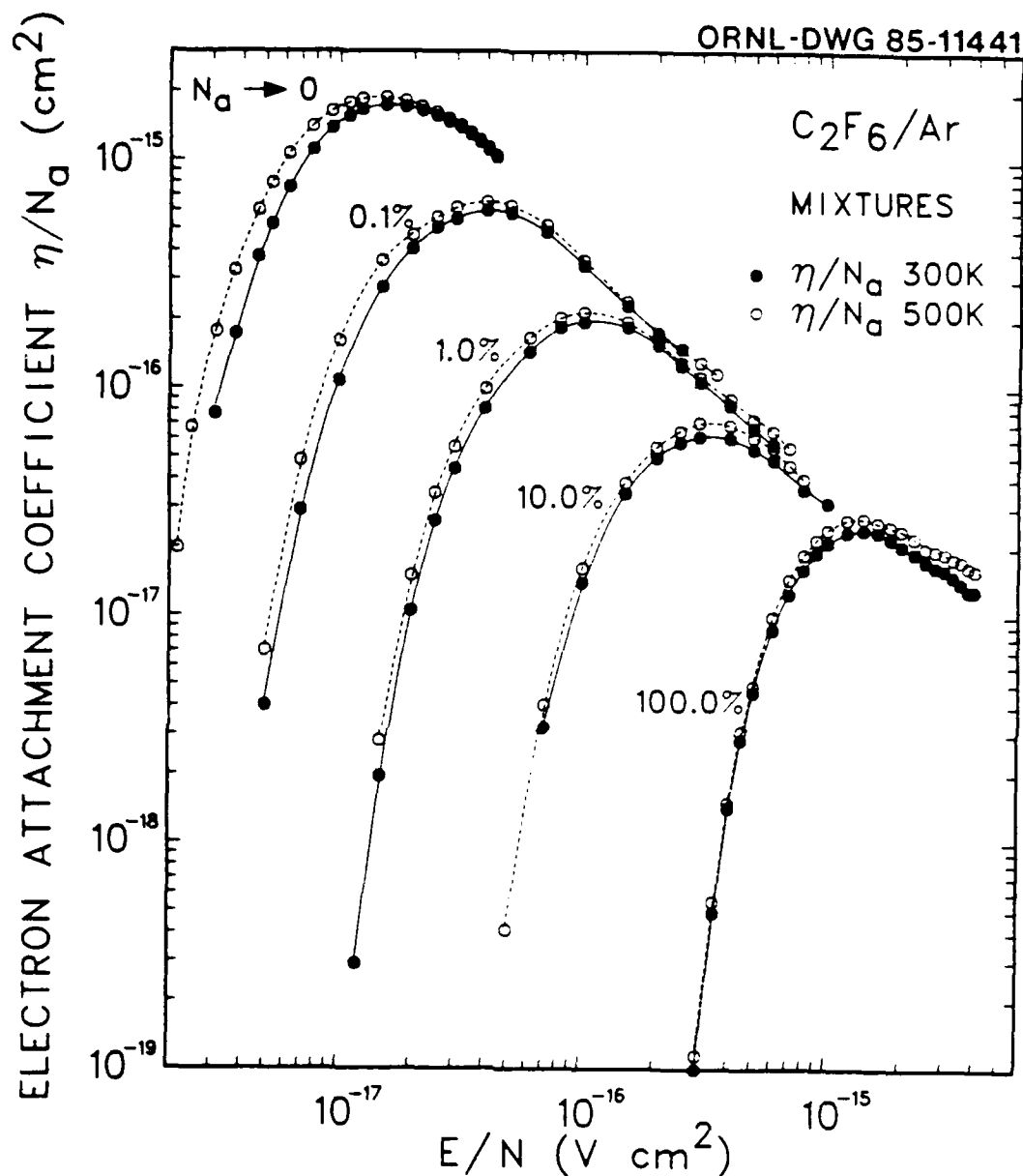


FIG. 2. Electron attachment coefficient η/N_a for several C₂F₆/Ar gas mixtures as a function of E/N at gas temperatures of 300 and 500 K. The measurements for $N_a \rightarrow 0$ are obtained from high pressure attachment rate constant measurements, where $\eta/N_a = k_a/w$ and N_a is very small (≈ 1 part in 10^6) compared with the buffer gas number density.

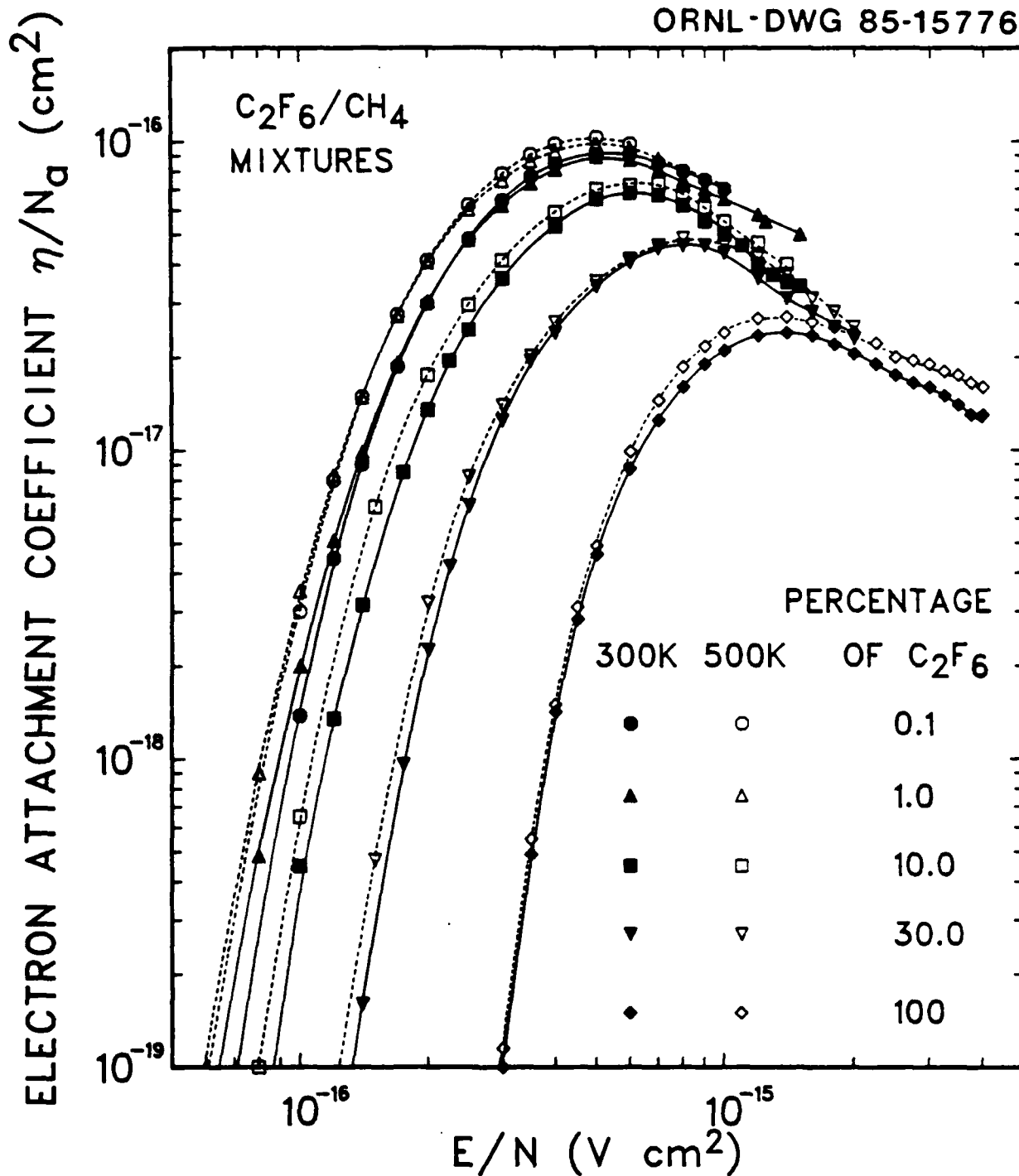


FIG. 3. Electron attachment coefficient η/N_a for several C_2F_6/CH_4 gas mixtures as a function of E/N at gas temperatures of 300 and 500 K. These measurements indicate that the attachment coefficient increases significantly at all concentrations of the attaching gas in the buffer gas for both the C_2F_6/Ar and C_2F_6/CH_4 gas mixtures.

ORNL-DWG 85-15779

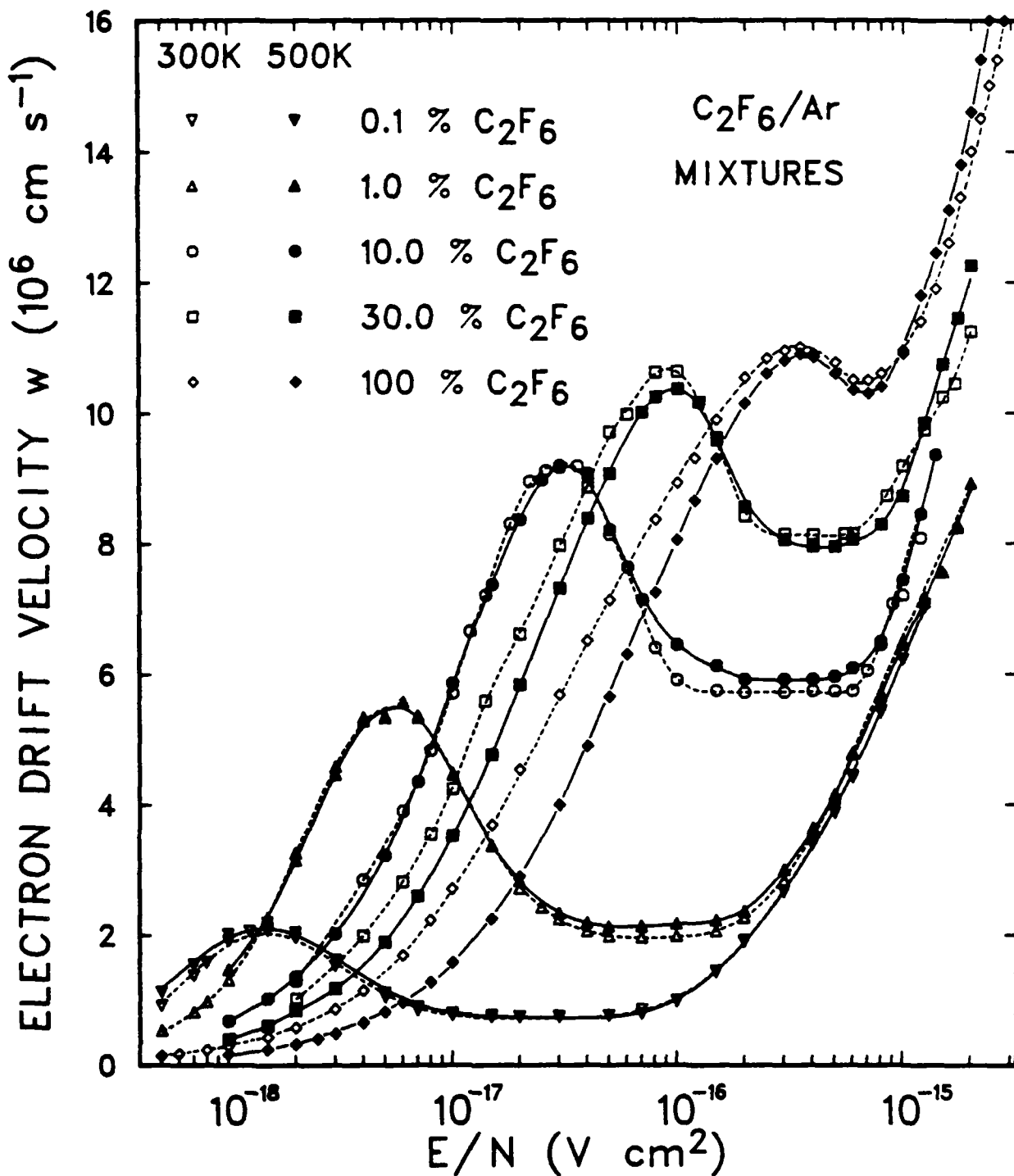


FIG. 4. Electron drift velocities as a function of E/N for several concentrations of C_2F_6 in Ar at gas temperatures of 300 and 500 K.

ORNL-DWG 85-15778

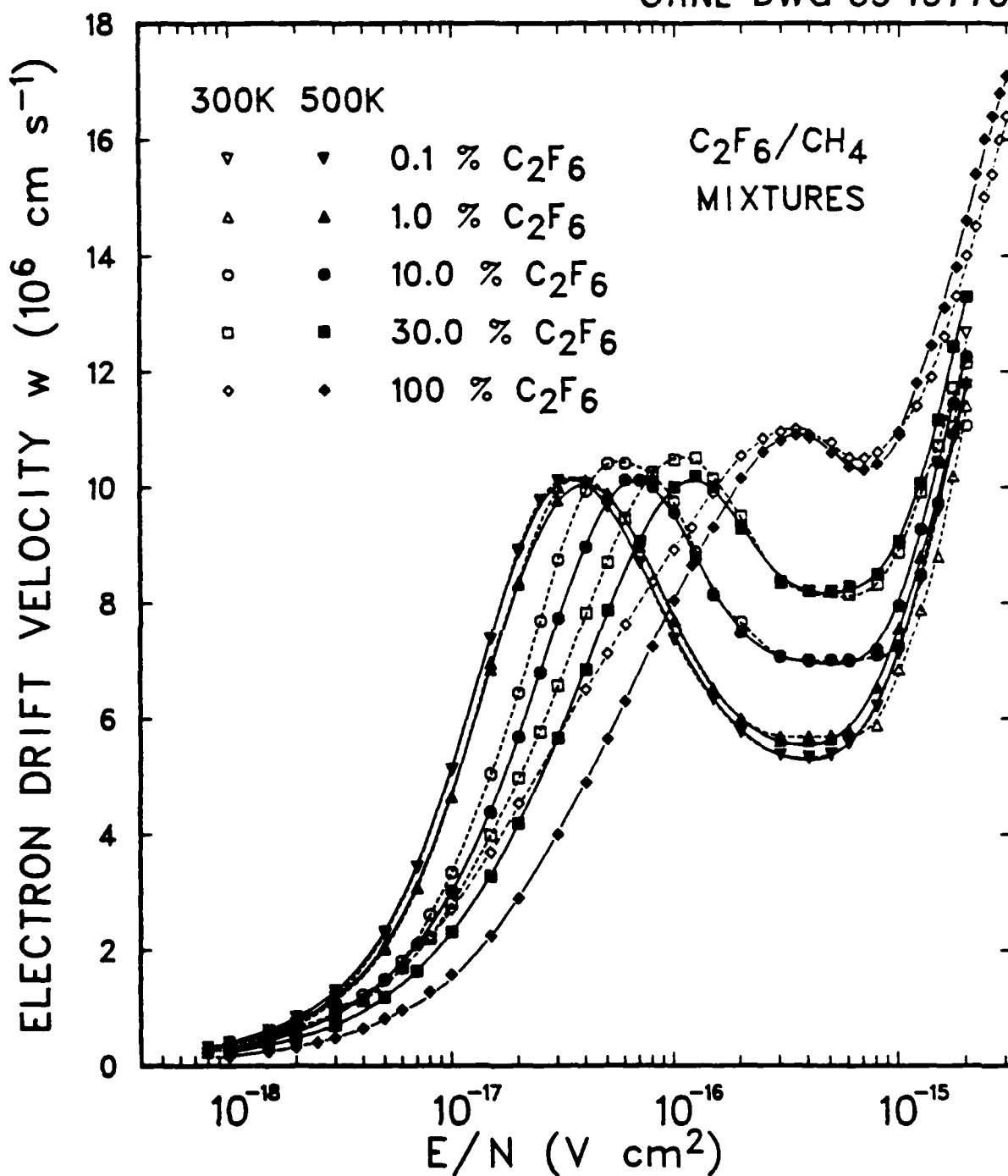


FIG. 5. Electron drift velocities as a function of E/N for several concentrations of C_2F_6 in CH_4 at gas temperatures of 300 and 500 K. The drift velocities are little affected by changes in the gas temperature at the higher E/N values near the peak in the electron drift in both the $\text{C}_2\text{F}_6/\text{Ar}$ and $\text{C}_2\text{F}_6/\text{CH}_4$ gas mixtures.

ORNL-DWG 85-15777

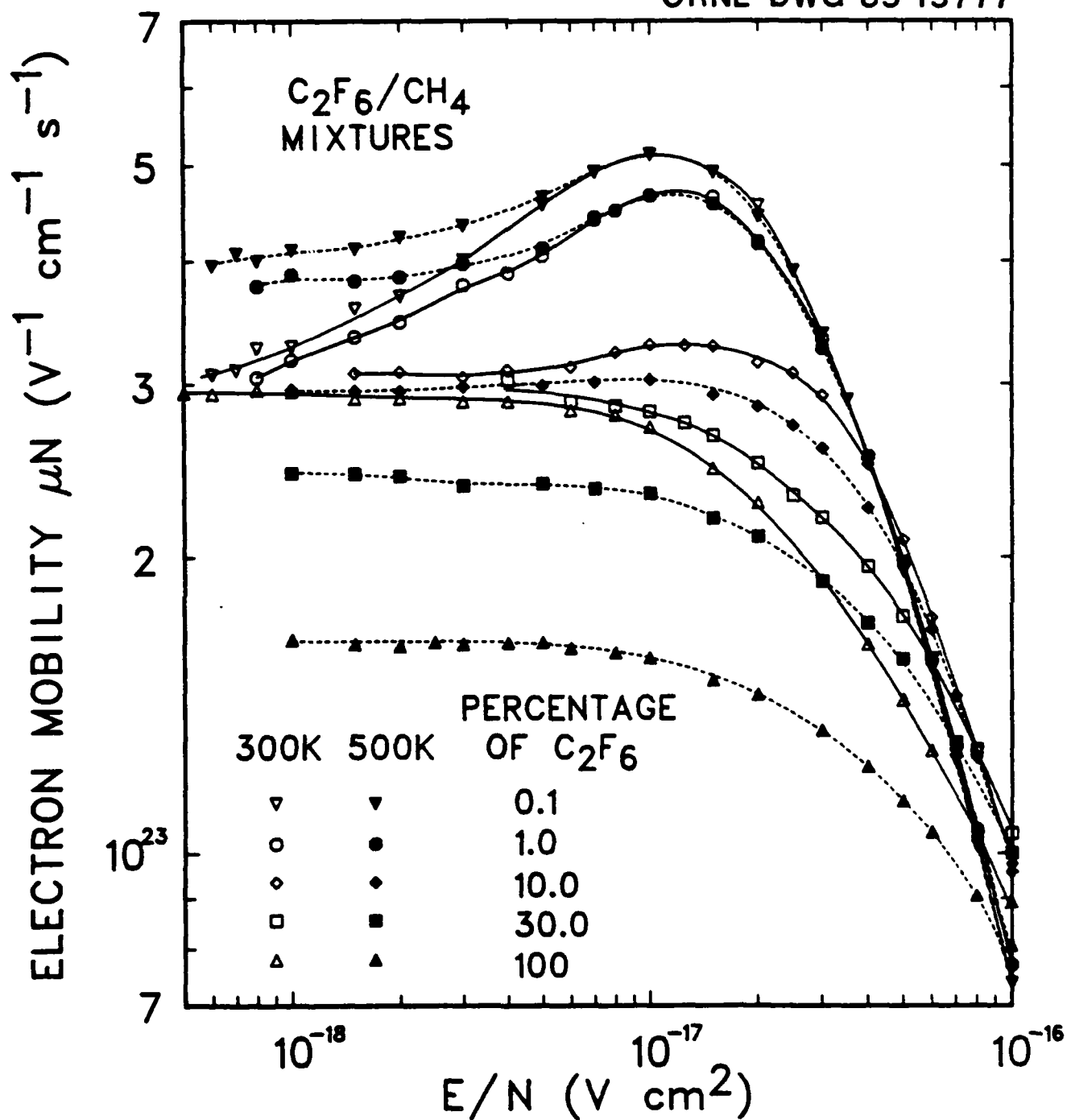


FIG. 6. The density normalized electron mobility μ_N in C_2F_6/CH_4 gas mixtures for low E/N values at gas temperatures of 300 and 500 K.

ORNL-DWG 85-15780

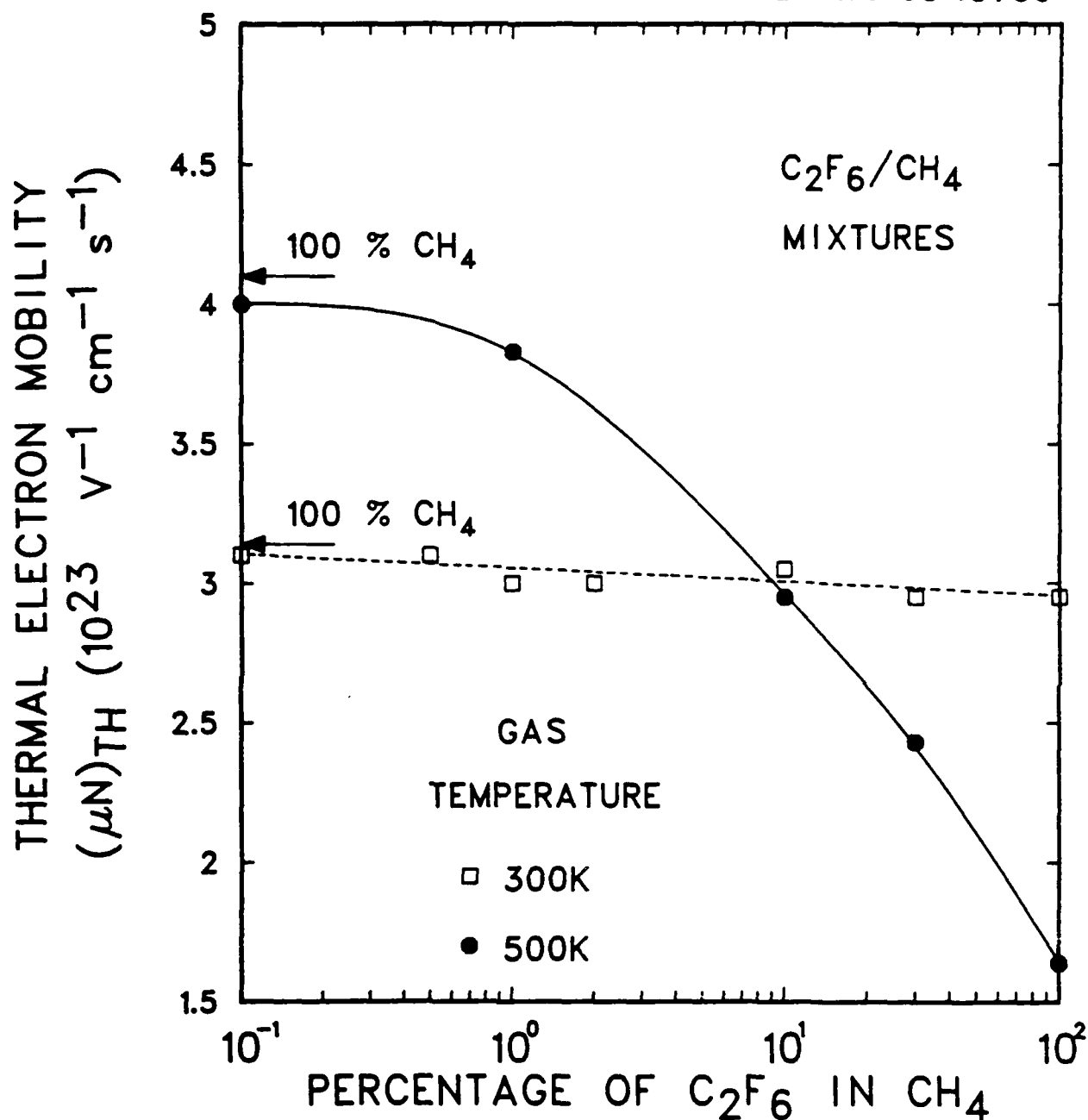


FIG. 7. Thermal electron mobilities in $\text{C}_2\text{F}_6/\text{CH}_4$ gas mixtures at gas temperatures of 300 and 500 K. At room temperature (300 K) the electron mobility is nearly independent of the concentration of the C_2F_6 in CH_4 . At higher gas temperatures, the electron mobility becomes a significant function of C_2F_6 concentration. Similar effects are seen in the $\text{C}_2\text{F}_6/\text{Ar}$ gas mixtures.

B. Publications

The majority of the measurements described above have been published or have been submitted for publication.¹⁻⁷ Our measurements of the electron attachment rate constants and negative ion production cross sections for the perfluoroalkanes, fluoroethers, and fluorosulfides have recently been published.⁸⁻¹⁰ Our high temperature electron attachment rate constant measurements to C_2F_6 and CCl_2F_3 ¹¹ and our high temperature k_a measurement in C_3F_8 have also been published recently.¹³ A paper has been written for journal publication in which our electron drift velocity, attachment, and ionization measurements in several proposed switching gas mixtures have been summarized, and the relevance of these results to the design and optimization of gas mixtures for diffuse discharge switching applications has been outlined.¹⁴ A paper has been published describing our initial W value measurements in C_2F_6 gas mixtures.¹² These measurements, analyses, and implications for diffuse gas discharge switching applications have been discussed in a paper which was presented at the 5th IEEE Pulsed Power Conference (Appendix A).¹⁶ An invited paper was also presented at this conference in which our measurements of the effect of gas temperature on the electron drift velocity and electron attaching and ionizing properties of gas molecules was discussed (see Appendix B).¹⁷

An invited paper describing the effects of elevated gas temperatures on the dissociative and nondissociative electron attachment properties of gas molecules, which have been observed under partial support by ONR, has been presented at the Joint Symposium on Swarm Studies and Inelastic Electron-Molecule Collisions (see Appendix C).²³

IV. REFERENCES

1. L. G. Christophorou, S. R. Hunter, J. G. Carter, and R. A. Mathis, Appl. Phys. Lett. 41, 147 (1982).
2. L. G. Christophorou, S. R. Hunter, J. G. Carter, and S. M. Spyrou, in Proceedings of Workshop on "Diffuse Discharge Opening Switches", The Texas Tech University Press, Lubbock, Texas, 1982, page 236.
3. S. R. Hunter and L. G. Christophorou, Bull. Am. Phys. Soc. 28, 185 (1983).
4. S. M. Spyrou and L. G. Christophorou, Bull. Am. Phys. Soc. 28, 185 (1983).
5. L. G. Christophorou, S. R. Hunter, J. G. Carter, S. M. Spyrou, and V. K. Lakdawala, in Proceedings of the 4th IEEE Pulsed Power Conference (M. F. Rose and T. H. Martin, Eds.), The Texas Tech University Press, Lubbock, Texas, 1983, page 702.
6. J. G. Carter, S. R. Hunter, L. G. Christophorou, and V. K. Lakdawala, in Proceedings of the 3rd International Swarm Seminar (W. Lindinger, H. Villinger, and W. Federer, Eds.), Innsbruck, Austria, 1983, page 30.
7. S. R. Hunter, J. G. Carter, L. G. Christophorou, and V. K. Lakdawala, in Gaseous Dielectrics IV (L. G. Christophorou and M. O. Pace, Eds.), Pergamon Press, New York, 1984, page 224.
8. S. M. Spyrou, I. Sauers, and L. G. Christophorou, J. Chem. Phys. 78, 7200 (1983).
9. S. R. Hunter and L. G. Christophorou, J. Chem. Phys. 80, 6150 (1984).
10. S. M. Spyrou, S. R. Hunter, and L. G. Christophorou, J. Chem. Phys. 81, 4481 (1984).

11. S. M. Spyrou and L. G. Christophorou, J. Chem. Phys. 82, 1048 (1985).
12. K. Nakanishi, L. G. Christophorou, J. G. Carter, and S. R. Hunter, J. Appl. Phys. 58, 633 (1985).
13. S. M. Spyrou and L. G. Christophorou, J. Chem. Phys. 83, 2829 (1985).
14. S. R. Hunter, J. G. Carter, and L. G. Christophorou, "Electron Transport Studies of Gas Mixtures for Use in e-Beam Controlled Diffuse Discharge Switches", Journal of Applied Physics (in press).
15. L. G. Christophorou, S. R. Hunter, J. G. Carter, and S. M. Spyrou, "Effect of Temperature on Dissociative and Nondissociative Electron Attachment", to be published in the Proceedings of the Joint Symposium on Swarm Studies and Inelastic Electron-Molecule Collisions, Tahoe City, California, July 19-23, 1985.
16. K. Nakanishi, L. G. Christophorou, J. G. Carter, and S. R. Hunter, "Penning Ionization Ternary Gas Mixtures for Diffuse Discharge Switching Applications", to be published in the Proceedings of the 5th IEEE Pulsed Power Conference, Arlington, Virginia, June 10-12, 1985.
17. S. R. Hunter, J. G. Carter, L. G. Christophorou, and S. M. Spyrou, "Temperature Dependent Electron Transport Studies for Diffuse Discharge Switching Applications", to be published in the Proceedings of the 5th IEEE Pulsed Power Conference, Arlington, Virginia, June 10-12, 1985.
18. I. Sauers, W. D. Evans, J. L. Adcock, and L. G. Christophorou, "Decomposition of CF_4/Ar Mixtures in Corona Discharges", to be published in the Proceedings of the 5th IEEE Pulsed Power Conference, Arlington, Virginia, June 10-12, 1985.

19. L. G. Christophorou, D. L. McCorkle, D. V. Maxey, and J. G. Carter, Nucl. Instr. Meth. 163, 141 (1979).
20. L. G. Christophorou, D. V. Maxey, D. L. McCorkle, and J. G. Carter, Nucl. Instr. Meth. 171, 491 (1979).
21. L. G. Christophorou, J. G. Carter, and D. V. Maxey, J. Chem. Phys. 76, 2653 (1982).
22. S. R. Hunter, J. G. Carter, and L. G. Christophorou, "Electron Attachment, Ionization, and Drift in CH_4 and the Perfluoroalkanes $\text{n-C}_N\text{F}_{2N+2}$ ($N = 1$ to 4)", to be published in the Proceedings of the Joint Symposium on Swarm Studies and Inelastic Electron-Molecule Collisions, Tahoe City, California, July 19-23, 1985.
23. L. G. Christophorou, S. R. Hunter, and J. G. Carter, "Effects of Temperature on Dissociative and Nondissociative Electron Attachment", to be published in the Proceedings of the Joint Symposium on Swarm Studies and Inelastic Electron-Molecule Collisions, Tahoe City, California, July 19-23, 1985.

APPENDIX A

PENNING IONIZATION TERNARY GAS MIXTURES FOR DIFFUSE DISCHARGE SWITCHING APPLICATIONS*

K. Nakanishi,[†] L. G. Christophorou,[†] J. G. Carter, and S. R. Hunter
Atomic, Molecular and High Voltage Physics Group
Health and Safety Research Division
Oak Ridge National Laboratory
Oak Ridge, Tennessee 37831

Summary

The increase in the total ionization produced by high energy α particles in Ar/C₂F₆ mixtures (which have conduction and insulation properties appropriate for use in diffuse discharge switching applications) by addition of low ionization energy additives has been quantitatively studied. The energy to produce an electron-ion pair (ip), W , in C₂F₆ was found to be 34.7 eV/ip; this rather high value is attributed to the large cross section for electron impact-induced dissociation of C₂F₆. The W values of Ar/C₂F₆ mixtures have also been measured and are reported; they increase with increasing C₂F₆ content. The W values of Ar/C₂F₆ binary gas mixtures have been found to decrease--higher total ionization--by addition of C₂H₂ or 2-C₄H₈. Quantitative measurements of the W values of the ternary gas mixtures are reported. The amounts of C₂H₂ or 2-C₄H₈ in Ar/C₂F₆ which maximize the increase in total ionization have been estimated; some of these ternary gas mixtures may be useful in e-beam-sustained diffuse discharge switches.

Binary and Ternary Gas Mixtures for Diffuse Discharge Switching Applications

Christophorou and coworkers¹⁻⁴ have shown that binary gas mixtures composed of buffer gases such as Ar and CH₄ whose electron scattering cross sections have a Ramsauer-Townsend minimum at low energies (at ~ 0.3 eV), and electron attaching gases such as CF₄, C₂F₆, and C₃F₈, which attach electrons efficiently at high density-reduced electric fields E/N and have much reduced electron attachment rate constants at low E/N , are most appropriate for diffuse discharge switching applications. Such mixtures have distinct maxima in the electron drift velocity, v , as a function of E/N at E/N values appropriate for the conducting stage of the switch; they have, at these E/N values, w values in excess of 10^7 cm s⁻¹ and breakdown strengths $>150 \times 10^{-17}$ V cm² for mixtures containing $\geq 10\%$ of the attaching gas.

In the present study we further optimize the conduction properties of such gas mixtures by reducing the energy required to produce an electron-ion pair, W , of the binary gas mixture (e.g., Ar/C₂F₆). This is achieved by adding to the Ar/C₂F₆ mixtures small amounts of low ionization energy additives such as C₂H₂ and 2-C₄H₈. Since the ionization energies of C₂H₂ and 2-C₄H₈ (~ 11.3 eV and ~ 9.2 eV,⁵ respectively) are lower than the excitation energies of Ar,⁵ the molecules C₂H₂ and 2-C₄H₈ are expected to be ionized by collisional energy transfer from excited argon atoms⁶ (i.e., via Penning ionization processes). The W values of C₂F₆, C₂H₂, 2-C₄H₈, Ar/C₂F₆, C₂F₆/C₂H₂, C₂F₆/2-C₄H₈, Ar/C₂F₆/C₂H₂, and

Ar/C₂F₆/2-C₄H₈ have been measured using high energy α particles and are reported. Since the energies of the electron beams normally used in diffuse discharge switching applications are in the keV range, the W values for α and β particles are expected to be similar.⁵ The W values of the ternary mixtures were found to be lower--total ionization higher--than the W values of the binary Ar/C₂F₆ mixtures, by an amount which depends both on the percentage of the additive to the binary gas mixture and the percentage of C₂F₆ in Ar.

Measurement of W

In Fig. 1 is shown the block diagram of the system we employed to measure W . An uncollimated Pu²³⁹ source was used which produced $\sim 6 \times 10^4$ α particles per second of initial energy ~ 5.1 MeV. For the pressures employed (≥ 100 kPa) the α particles were completely stopped in the gaseous medium. The principle of the measurement is described in Ref. 8 (see also Ref. 9). Briefly, when the switch (Fig. 1) is closed (contact 2 closed), electrons and ions created by the α particle energy decay in the gas produce a current in the collector circuit which is collected as charge on the low loss capacitor C . Simultaneously, an electrical stopwatch starts counting the time by closing relay 1. The ramped generator in the circuit was used as a source of bucking voltage to the capacitor. The voltage of the ramped generator was controlled through a feedback circuit by the output of a high impedance voltmeter ($\sim 10^{14}$ Ω) which monitored the potential between X and Y (see Fig. 1).

The charge Q collected at the capacitor is expressed as the product of the capacitance C and the voltage across the capacitor V . The number, n , of ion pairs produced per second is then given by

$$n = (1/e)(dQ/dt) = (C/e)(dV/dt), \quad (1)$$

where e is the electron charge. The total energy deposited in the gas per second by the α particles is $\epsilon_0 N_0$, where ϵ_0 is the energy of each α particle and N_0 is the number of α particles which are completely stopped in the gas per second. Since W is the average energy required to produce an ion pair, it is equal to

$$W = \epsilon_0 N_0 / n = \epsilon_0 N_0 / (C/e)(\Delta V/\Delta t). \quad (2)$$

*Research sponsored in part by the Office of Naval Research under contract 43 01 24 60 2 and in part by the Division of Electric Energy Systems, U.S. Department of Energy, under contract DE-AC05-84OR21400 with Martin Marietta Energy Systems, Inc.

[†]Permanent address: Central Research Laboratory, Mitsubishi Electric Corporation, 8-1-1 Tsukaguchi Hommachi, Amagasaki, Japan

[†]Also, Department of Physics, The University of Tennessee, Knoxville, Tennessee 37996.

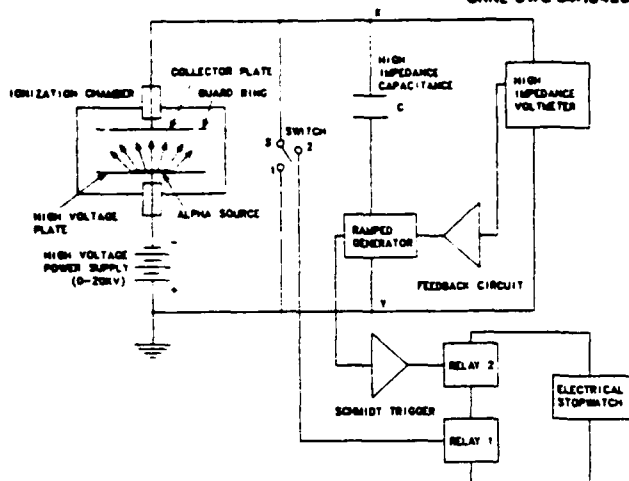


Fig. 1. Schematic diagram of the apparatus for measurement of the W values.

Since in Eq. (2) C , ϵ_0 , and N_0 are constant during the experiment, the W value can be determined by measuring ΔV and Δt for the gas under investigation and comparing these values with those for a reference standard gas. In the present experiments, we measured the time Δt required to charge C to a fixed value (1.824 V) which was the threshold voltage of the Schmitt trigger circuit. When the voltage across the capacitor reached the fixed voltage, the electrical stopwatch was stopped by the signal from the Schmitt circuit (i.e., relay 2 was opened). Since the W value for pure argon is well known (26.4 eV/ip³), we used Ar as the standard reference gas in our study. The unknown W value for the gas mixture, W_m , was obtained from

$$W_{Ar}/\Delta t_{Ar} = W_m/\Delta t_m \quad (3)$$

using the measured times Δt_{Ar} and Δt_m required to charge C to a fixed value when the chamber was filled, respectively, with Ar and the gas mixture. Since C_2F_6 is an electronegative gas, for pure C_2F_6 or for C_2F_6 mixtures containing high concentrations of C_2F_6 , the W measurement was affected by positive ion-negative ion recombination. For such systems we measured W as a function of pressure and applied voltage. At each pressure, plots of W^{-1} versus V^{-1} extrapolated [for $V^{-1} \rightarrow 0$ (i.e., $E/N \rightarrow \infty$)] to a common W value free of recombination effects (see further details in Ref. 8).

W Values

The W values for C_2F_6 , C_2H_2 , and $2-C_4H_8$ and the binary mixtures of C_2F_6 with either Ar or C_2H_2 or $2-C_4H_8$ are shown in Fig. 2. The binary mixtures of C_2F_6 do not show a "Jesse effect"⁵ [i.e., an abrupt decrease in W (the W value of the mixture) as small amounts of $2-C_4H_8$ or C_2H_2 are added to C_2F_6 , due to Penning ionization], although a number of excited electronic states of C_2F_6 exist¹⁰ above the ionization energies of C_2H_2 and $2-C_4H_8$. The behavior of the C_2F_6 -containing binary gas mixtures is in contrast to that of the binary gas mixtures Ar/ $2-C_4H_8$ and Ar/ C_2H_2 which showed a Jesse effect;^{5,9} it is attributed⁸ to the fast dissociation of the electronically excited C_2F_6 molecules.⁷

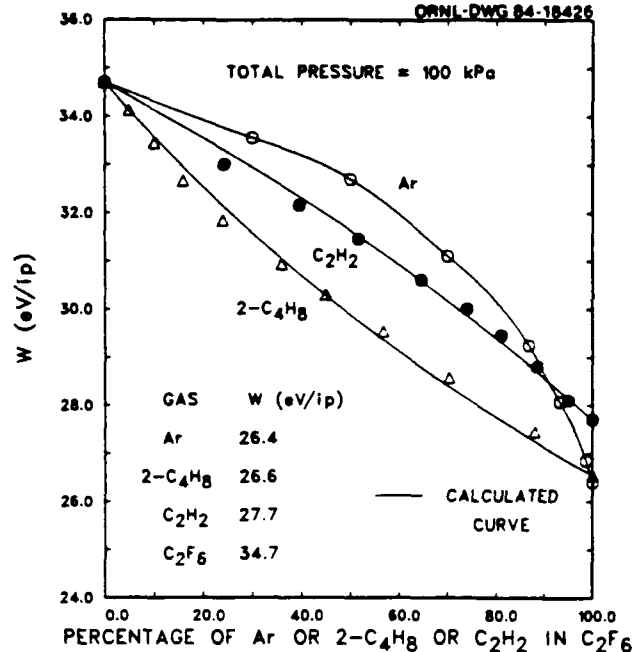


Fig. 2. Experimental W values of Ar/ C_2F_6 , $2-C_4H_8/C_2F_6$, and C_2H_2/C_2F_6 gas mixtures as a function of the percentage of Ar, $2-C_4H_8$, or C_2H_2 in C_2F_6 and their comparison with the calculated data. The symbols are the experimental values; the lines are the calculated results (see Ref. 8).

The experimental W values of the ternary gas mixtures Ar/ C_2F_6 /X were measured at a total pressure of 100 kPa and are shown in Figs. 3 and 4. They were obtained by adding the impurity gas X (C_2H_2 or $2-C_4H_8$) to the Ar/ C_2F_6 mixtures having the following composition ratios: 4/1; 9/1; 19/1; 49/1; and 99/1. It is seen that addition of X to the Ar/ C_2F_6 mixture decreases W (increases ionization) considerably. The decrease in the W of the ternary mixture goes through a minimum for ternary mixtures containing $\leq 10\%$ C_2F_6 in the Ar/ C_2F_6 binary component. The smaller the percentage of C_2F_6 in the binary Ar/ C_2F_6 mixture used, the lower the concentration of C_2H_2 or $2-C_4H_8$ in the respective ternary gas mixture for which the minimum value of W (maximum ionization) is realized. The observed increase in W with increasing C_2F_6 /Ar ratio is considered to be due to the quenching of the excited argon atoms by C_2F_6 leading to the dissociation of the latter; this quenching process competes with the Penning ionization process involving excited argon atoms and ground state X molecules.

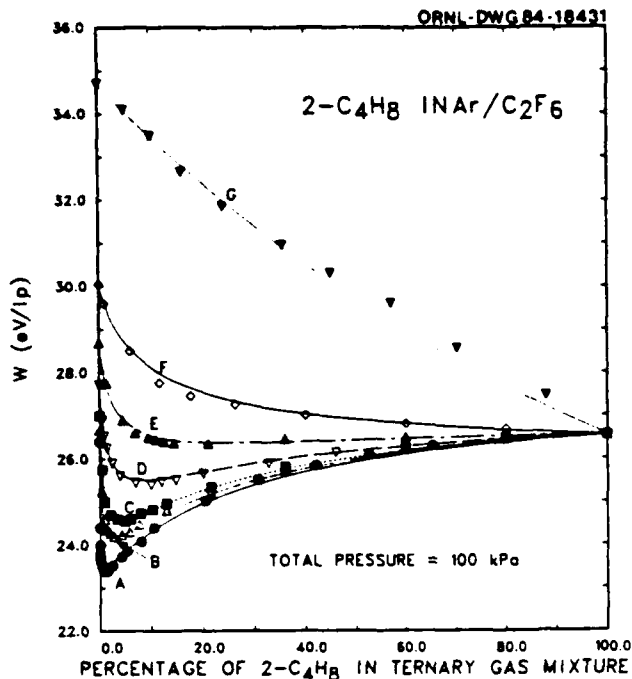


Fig. 3. Experimental W values of $\text{Ar}/\text{C}_2\text{F}_6/2\text{-C}_4\text{H}_8$ ternary gas mixtures as a function of the percentage of $2\text{-C}_4\text{H}_8$ in the $\text{Ar}/\text{C}_2\text{F}_6$ mixtures, having the following compositions: A, $\text{Ar}/\text{C}_2\text{F}_6 = 1/0$; B, $\text{Ar}/\text{C}_2\text{F}_6 = 99/1$; C, $\text{Ar}/\text{C}_2\text{F}_6 = 49/1$; D, $\text{Ar}/\text{C}_2\text{F}_6 = 19/1$; E, $\text{Ar}/\text{C}_2\text{F}_6 = 9/1$; F, $\text{Ar}/\text{C}_2\text{F}_6 = 4/1$; G, $\text{Ar}/\text{C}_2\text{F}_6 = 0/1$. The symbols are the experimental values, and the lines are the calculated values using Eq. (4) (see Ref. 8 for details).

Modeling of the Data

A theoretical analysis of the W data for the ternary $\text{Ar}/\text{C}_2\text{F}_6/\text{X}$ mixtures has led to the expression⁸

$$\frac{1}{W_m} = \left(\frac{1}{W_A} - \frac{1}{W_C} \right) \frac{P_A}{P_A + \left(\frac{k_2}{k_1} \right) P_C + \left(\frac{k_3}{k_1} \right) P_X} + \left(\frac{1}{W_X} - \frac{1}{W_C} \right) \frac{\left(\frac{k_3}{k_1} \right) P_X}{P_A + \left(\frac{k_2}{k_1} \right) P_C + \left(\frac{k_3}{k_1} \right) P_X} + \frac{1}{W_C} + \alpha \frac{P_A}{P_A + \left(\frac{k_2}{k_1} \right) P_C + \left(\frac{k_3}{k_1} \right) P_X} \frac{P_X}{P_X + \left(\frac{c_2}{c_1} \right) P_A + \left(\frac{c_3}{c_1} \right) P_X} \quad (4)$$

where W_A , W_C , and W_X , and P_A , P_C , and P_X are, respectively, the W values and the partial pressures of Ar , C_2F_6 and X (C_2H_2 or $2\text{-C}_4\text{H}_8$); k_1 , k_2 , k_3 , c_1 , c_2 , and c_3 are the rate constants for the respective reactions below:

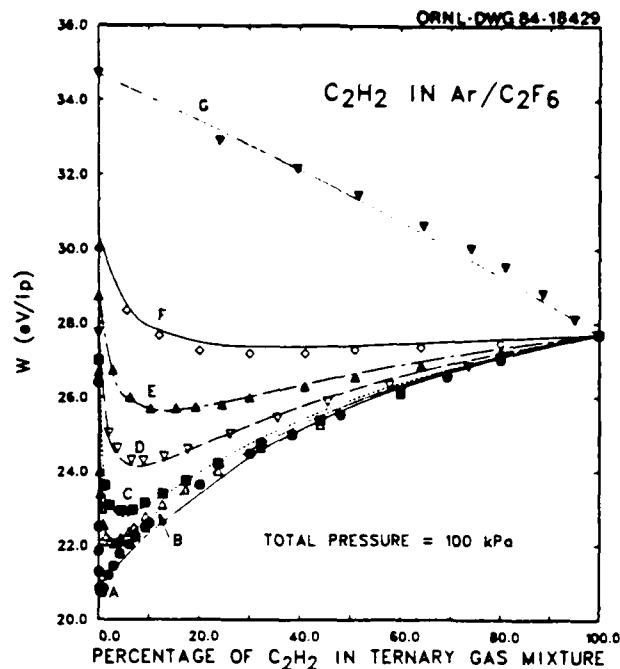
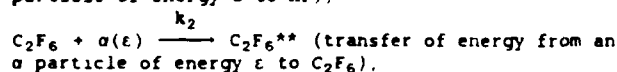
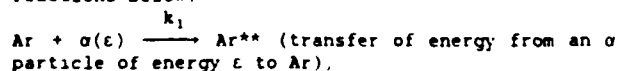
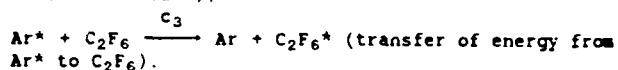
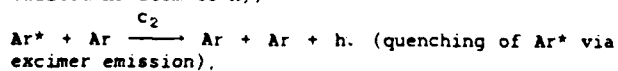
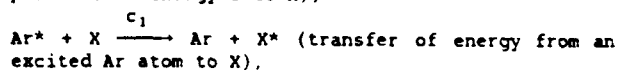
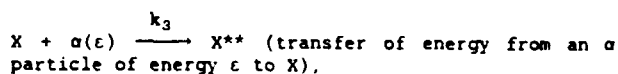


Fig. 4. Experimental W values of $\text{Ar}/\text{C}_2\text{F}_6/\text{C}_2\text{H}_2$ ternary gas mixtures as a function of the percentage of C_2H_2 in $\text{Ar}/\text{C}_2\text{F}_6$ mixtures having the following compositions: A, $\text{Ar}/\text{C}_2\text{F}_6 = 1/0$; B, $\text{Ar}/\text{C}_2\text{F}_6 = 99/1$; C, $\text{Ar}/\text{C}_2\text{F}_6 = 49/1$; D, $\text{Ar}/\text{C}_2\text{F}_6 = 19/1$; E, $\text{Ar}/\text{C}_2\text{F}_6 = 9/1$; F, $\text{Ar}/\text{C}_2\text{F}_6 = 4/1$; G, $\text{Ar}/\text{C}_2\text{F}_6 = 0/1$. The symbols are the experimental values, and the lines are the calculated values using Eq. (4) (see Ref. 8 for details).



In Eq. (4), $\alpha = \xi_1(1-\eta_1)/\epsilon_A$, where ξ_1 is the probability of ionization of X by energy transfer from Ar^* , $(1-\eta_1)$ is the probability of formation of Ar^* when an α particle of energy ϵ collides with Ar , and ϵ_A is the average excitation energy of Ar .

Through a nonlinear least squares fitting routine,⁸ we found the values of k_2/k_1 , k_3/k_1 , c_2/c_1 , c_3/c_1 , and α using the data in Figs. 3 and 4 for $\text{Ar}/\text{C}_2\text{F}_6/\text{C}_2\text{H}_2$ and $\text{Ar}/\text{C}_2\text{F}_6/2\text{-C}_4\text{H}_8$. The values of these parameters are given in Table 1 and have been used in Eq. (4) to obtain the calculated (solid) curves in Figs. 3 and 4. The calculated and the experimental data agree well for both of the ternary mixtures indicating that our model is able to satisfactorily account for the observed partial pressure dependences of W_m in these gas mixtures. The values of the ratios k_2/k_1 , k_3/k_1 , c_2/c_1 , and α were also calculated from the data in the binary gas mixtures and are also given in Table 1. They generally agree with those calculated in the ternary gas mixtures to better than 10%, which is the order of magnitude of the calculated standard deviations for these

parameters. Consequently, we expect that these parameters are accurate to within this error limit and can be used to determine optimum gas mixture compositions when maximum enhancement of the Penning gas ionization processes is desirable.

TABLE 1 The parameters calculated in a nonlinear least squares fit to the experimental data in the binary and ternary gas mixtures

Binary gas mixtures - no Penning ionization			
	C_2F_6/Ar	$C_2F_6/2-C_4H_8$	C_2F_6/C_2H_2
k_2/k_1	4.25 ± 0.12	0.90 ± 0.03	1.60 ± 0.06
Binary gas mixtures - with Penning ionization			
	$2-C_4H_8/Ar$	C_2H_2/Ar	
k_3/k_1	5.08 ± 0.28	3.93 ± 0.25	
C_2/C_1	$(1.86 \pm 0.16) \times 10^{-4}$	$(1.39 \pm 0.19) \times 10^{-4}$	
α	$(5.16 \pm 0.06) \times 10^{-3}$	$(1.04 \pm 0.02) \times 10^{-2}$	
Ternary gas mixtures - with Penning ionization			
	$2-C_4H_8/Ar/C_2F_6$	$C_2H_2/Ar/C_2F_6$	
k_2/k_1	3.99 ± 0.10	4.72 ± 0.13	
k_3/k_1	4.83 ± 0.18	3.32 ± 0.09	
C_2/C_1	$(1.76 \pm 0.21) \times 10^{-4}$	$(1.24 \pm 0.13) \times 10^{-4}$	
C_3/C_1	0.397 ± 0.028	0.384 ± 0.020	
α	$(5.13 \pm 0.07) \times 10^{-3}$	$(1.02 \pm 0.01) \times 10^{-2}$	

Conclusions

We obtained, for the first time, quantitative data on the W values of C_2F_6 and Ar/C_2F_6 mixtures which are of interest to diffuse discharge switching applications. Additionally, we have shown that the total ionization produced in the Ar/C_2F_6 mixtures by the external particle beam can be considerably increased by addition of small amounts of a low ionization energy additive such as C_2H_2 or $2-C_4H_8$ to the Ar/C_2F_6 mixtures. This can be seen from Figs. 3 and 4 and from the data in Table 2. It can, for instance, be seen that the W value of a 99% $Ar/1\% C_2F_6$ mixture is reduced from 26.7 eV/ip to 22.1 eV/ip by the addition of 3% of C_2H_2 . The increase in ionization is, of course, a function of both the relative amounts of C_2F_6 in the ternary mixture and the nature of the additive X. While other additives besides the ones we used can be employed, these must not attach slow electrons (this is the case for both C_2H_2 and $2-C_4H_8$) and must not adversely affect the drift velocity maxima which characterize the binary Ar/C_2F_6 mixtures.¹⁻⁴

TABLE 2 W values for Ar/C_2F_6 mixtures as a function of their composition. minimum value of W when $2-C_4H_8$ or C_2H_2 is added to these and percentage of $2-C_4H_8$ or C_2H_2 for which W_{min} is realized in the ternary mixtures

Composition of Ar/C_2F_6 mixtures	W_{Ar/C_2F_6} (eV/ip)	W_{min} of $Ar/C_2F_6/X$		% of X at which W_{min} occurs	
		$2-C_4H_8$	C_2H_2	$2-C_4H_8$	C_2H_2
100	26.4	20.4	20.8	1.3	0.5
99	26.7	24.2	22.1	3.5	3.0
49	27.0	24.5	22.9	4.9	5.3
19	27.6	25.4	24.3	9.5	8.5
9	28.7	26.1	25.7	19.0	13.5
4	30.1	-	27.1	-	36.0
1	34.7	-	-	-	-

References

1. L. G. Christophorou, S. R. Hunter, J. G. Carter, and R. A. Mathis, *Appl. Phys.* **41**, 147 (1982).
2. L. G. Christophorou, S. R. Hunter, J. G. Carter, S. M. Spyrou, and V. K. Lakdawala, in *Proc. 4th IEEE Pulsed Power Conf.* (The Texas Tech Press, Lubbock, Texas, 1983), p. 702.
3. J. G. Carter, S. R. Hunter, L. G. Christophorou, and V. K. Lakdawala, in *Proc. 3rd Int. Swarm Seminar* (Innsbruck, Austria, 1983), p. 30.
4. S. R. Hunter, J. G. Carter, L. G. Christophorou, and V. K. Lakdawala, in *Gaseous Dielectrics IV* (Pergamon Press, New York, 1984), p. 224.
5. L. G. Christophorou, *Atomic and Molecular Radiation Physics* (Wiley-Interscience, New York, 1971).
6. Since the ionization energy of C_2F_6 is 14.6 eV, a number of electronically excited states of C_2F_6 lie above the ionization energy of the additives. However, no Penning ionization of the additives through collisions with excited C_2F_6 molecules is expected since the electronically excited C_2F_6 molecules undergo rapid dissociation (e.g., see Ref. 7).
7. H. F. Winters and M. Inokuti, *Phys. Rev.* **25**, 1420 (1982).
8. K. Nakanishi, L. G. Christophorou, J. G. Carter, and S. R. Hunter, *Journal of Applied Physics* (in press).
9. T. E. Bortner, G. S. Hurst, M. Edmundson, and J. E. Parks, Oak Ridge National Laboratory Report ORNL-3422 (1955).
10. M. B. Robin, *Higher Excited States of Polyatomic Molecules*, Vol. 1 (Academic Press, New York, 1974), p. 188.

APPENDIX B

S. R. Hunter, J. G. Carter, L. G. Christophorou,[†] and S. M. Spyrou[‡]
 Atomic, Molecular and High Voltage Physics Group
 Health and Safety Research Division
 Oak Ridge National Laboratory
 Oak Ridge, Tennessee 37831

Summary

A diffuse gas discharge switch must be capable of high speed, repetitive switching (i.e., switching times $<10^{-6}$ s; repetition rates up to 10^4 Hz; lifetimes up to 10^7 shots) without significant degradation of its electron conduction and opening characteristics if it is to be useful in pulsed power switching applications. Whenever the switch is fired, the gas temperature T within the switch is expected to rise several degrees centigrade, and operating temperatures of several hundred degrees are likely for repetitively operated switches. The electron transport and rate coefficients, such as the electron drift velocity and the electron attachment coefficient for the most promising gas mixtures under study are expected to be functions of T , and consequently, knowledge of these parameters as a function of T is desirable for modeling the operation of the diffuse discharge switch in practical application. Measurements of these parameters in C_2F_6 /buffer gas (Ar , CH_4 , N_2) mixtures have been made and are reported. The electron attachment rate constant has also been measured for C_2F_6 and C_3F_8 as a function of the mean electron energy $\langle \epsilon \rangle$ ($0.7 \leq \langle \epsilon \rangle \leq 5$ eV) over the temperature range $300 \leq T \leq 750$ K. For C_2F_6 , the electron attachment rate constant has been found to increase by 30% over this temperature range, while for C_3F_8 , the attachment rate constant first decreases when the temperature is increased to ~ 450 K and then significantly increases with increasing T . An interpretation of these measurements and their significance in repetitively operated diffuse discharge switching gas mixtures is outlined.

Introduction

Externally controlled diffuse gas discharges show considerable promise for use as switches where one wishes to rapidly transfer electrical energy from an inductive energy storage device to a load on a repetitive basis. The gas discharge within the switch can be controlled either by volume ionization of the gas by a high energy pulsed electron beam (e-beam controlled) or by resonance ionization of the gaseous medium using a pulsed high power UV laser (optically controlled). In both cases, the electric field across the switch during conduction must be sufficiently low, such that the discharge is completely controlled by the external electron source.

Several operating parameters may be defined for diffuse discharge opening switches, most of which are common to both e-beam and optically controlled diffuse discharges. Knowledge of these parameters can then form a basis for tailoring specific gases

and gas mixtures to optimize the switch operating conditions as nearly as possible. The relevant basic physical quantities include the electron attachment, recombination, ionization and diffusion coefficients, and the electron drift velocity as a function of E/N (the electric field strength E to gas number density N ratio), N and gas temperature T ; the energy needed to produce an electron-positive ion pair W ; and the high voltage breakdown field strengths of these gas mixtures. Studies of these transport and rate coefficients at room temperature (~ 300 K) in several promising gas mixtures have recently been completed.^{1,2}

Very little work has been performed to date on repetitively operated diffuse gas discharges for switching applications.^{3,4} The few studies that have been made indicate that the current switching and high voltage breakdown characteristics of the gas mixtures are seriously affected by the frequency of operation of the switch.^{4,5} Under these circumstances it is necessary to know how a given gas mixture will behave in a repetitively operated switch and what are the upper limits on the switch repetition rate and the maximum number of switching operations that can be performed before the transport, and hence switching, characteristics of the gas mixture in the switch are seriously altered.

A preliminary study of the time dependence of the recovery process within the gas mixture after the operation of the switch has been made by DeWitt.⁶ He identified several mechanisms which control the rate at which the gas mixture recovers its original behavior. For short time intervals ($<10^{-6}$ s) after the switch has opened, large positive and negative ion and, to a smaller extent, electron number densities exist in the discharge channel between the switch electrodes. In this situation, the electric field in the discharge channel is large and highly distorted due to the presence of the ionic species. The gas temperatures are very high ($T \approx 30,000$ K) with large fractions of the neutral and ionic species in highly excited vibrational and electronic levels, and the gas number density in the discharge channel is correspondingly low. Considerable fragmentation of the gas constituents is also expected at early times ($<10^{-6}$ s), and these radicals may subsequently recombine to form the original molecules or new species.

The rapidity with which the gas mixture recovers to its initial properties is dependent upon a number of processes within the discharge. At early times ($<10^{-6}$ s), recovery is dependent upon the recombination rates of the various ionic and neutral species in the discharge channel. The rates for collisional and radiative quenching of the vibrational and

*Research sponsored in part by the Office of Naval Research under contract 43 01 24 60 2 and in part by the Office of Health and Environmental Research, U.S. Department of Energy under contract DE-AC05-84OR21400 with Martin Marietta Energy Systems, Inc.

[†]Also, Department of Physics The University of Tennessee, Knoxville, Tennessee 37996.

[‡]Present address: Theoretical and Physical Chemistry Institute, The National Hellenic Research Foundation, 48, Vassileos Constantinou Avenue, Athens 501/1, Greece.

metastable excited states are important at early times. The return to true thermal equilibrium at later times ($t > 10^{-5}$ s) is controlled by the drift and diffusion of the ionic species, and the transfer of the gas kinetic energy out of the discharge channel, and ultimately into the electrodes and walls of the switching device.

The time domain we are probing in our present experiments is the final fraction of the switch recovery transient where the gas temperatures are within a few hundred degrees C of ambient (~ 300 K). This region of the gas recovery process is the most crucial for switching studies in that high repetition rate ($< 10^3$ s $^{-1}$) switching will occur in this region, and it is vital to know how close to true thermal equilibrium the gas mixture need recover in order to regain its full switching capabilities.

An understanding of the factors that affect the operation of the switch under these conditions can be obtained by performing the electron transport and rate coefficient measurements at gas temperatures above room temperature. The higher the gas temperature at which the measurements can be performed, the earlier the fundamental processes controlling the gas recovery can be probed after a switching impulse. In this paper, measurements are given of the electron drift velocity w , attachment coefficient η/N_a , and ionization coefficient α/N_a (where N_a is the attaching gas number density) in C_2F_6/Ar gas mixtures at 300 and 500 K, and the electron attachment rate constant as a function of $\langle \epsilon \rangle$, $k(\langle \epsilon \rangle)$, for C_2F_6 and C_3F_8 at gas temperature up to 750 K. These results may be used to understand the influence of elevated gas temperatures on the repetitive operation of the diffuse gas discharge.

These experiments have been performed in conjunction with two other studies which have been reported on earlier in these proceedings.^{7,8} Studies have been performed to optimize the gas ionization efficiency (i.e., to reduce the energy required to produce an electron-positive ion pair, W) of the high energy e-beam in practical switching gas mixtures.⁷ In another study, the effects of gas decomposition have been simulated using low current corona gas discharges.⁸ This study has shown the impurities that are likely to occur in repetitively operated gas discharges and indicated ways in which the buildup of these impurities can be minimized.

Operating Parameters of a Diffuse Gas Discharge Opening Switch

It is possible to establish several requirements of a gas mixture in the diffuse gas discharge which will optimize the performance of the switch. The conductivity of the discharge must be maximized while the switch is conducting (i.e., the voltage drop, and hence the E/N , across the discharge should be low ($E/N < 3 \times 10^{-17}$ V cm 2) to minimize power losses and, consequently, gas heating effects in the switch). The opening time of the switch must be as short as possible (i.e., largest rate of decrease in the discharge current) once the e-beam has been switched off in order to maximize the voltage developed across the inductive energy storage device. Consequently, the electron conductivity in the discharge must be maximized during the opening stage, and the gas mixture must be able to withstand high transient voltage levels ($E/N > 10^{-15}$ V cm 2) while the switch is opening.

These operating conditions allow us to define several desirable characteristics of the gaseous medium in the conducting (low E/N) and opening (high

E/N) stages of the switching action. In the conducting stage, the requirements are:

1. Maximum electron drift velocity w ($> 10^7$ cm s $^{-1}$).
2. Minimum e-beam "ionization energy" W .
3. Minimum electron loss due to attachment and electron-positive ion recombination.
4. Minimum ionization rate constant k_i (the conductivity of the gas discharge is required to be completely controlled by the external ionization source, otherwise the opening time of the switch will be considerably increased due to additional gas ionization when the e-beam is switched off).

In the opening stage, the requirements of the gas mixture are as follows:

1. Minimum electron drift velocity w .
2. Maximum electron attachment rate constant k_a .
3. High breakdown strength E/N_{lim} ($> 10^{-15}$ V cm 2).
4. Self-healing gas mixtures for closed cycle operation.
5. In photoexcited and photoionized gas discharges (required for laser-controlled discharges) it is desirable to have an electron attaching gas in which electron attachment can be increased by photoexcitation of the molecules by the laser radiation.^{9,10}

The desirable characteristics for the E/N dependence of w and k_a for the gas mixture in the diffuse discharge are shown in Fig. 1.^{11,12}

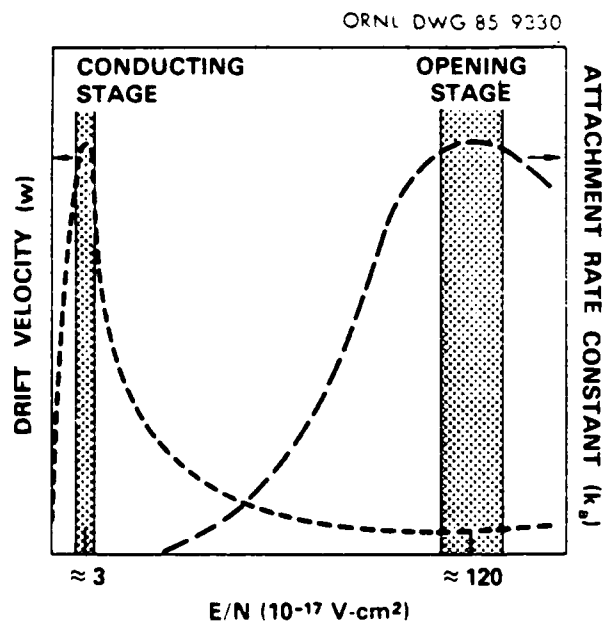


Fig. 1. Schematic illustration of the electron attachment rate constant $k_a(E/N)$ and the electron drift velocity $w(E/N)$ characteristics required of a gas mixture for use in a diffuse discharge opening switch. Approximate values of E/N for the discharge in the conducting and opening stages of the switch are shown in the figure (from Ref. 11).

Electron drift velocity measurements have been performed by us in a number of gas mixtures at room temperature and have been reported elsewhere.¹ All these gas mixtures have been found to exhibit maxima in w at low E/N values and a region of decreasing w with increasing E/N at higher electric fields [called a region of negative differential conductivity (NDC)] which, as shown in Fig. 1, is very desirable for diffuse discharge switching applications. In this paper, we report our present measurements in C_2F_6 /buffer gas mixtures at room temperature as these gas mixtures were used in our high temperature electron drift and attachment studies and were chosen as being representative of this class of gas mixtures as a whole.

Electron drift velocity measurements in C_2F_6 /Ar and C_2F_6 / CH_4 gas mixtures are given in Figs. 2 and 3, respectively, over the concentration range of 0 to 100% of the attaching gas in the buffer gas. These gas mixtures, along with the other gas mixtures given in Ref. 1, all possess pronounced regions of NDC over a range of E/N values. The NDC effects observed in several of these gas mixtures are among the largest that have been observed in any gas mixture and are the result of large vibrational inelastic energy loss processes in these electronegative gases at comparatively low electron energies [$0.1 < \epsilon \leq 1.0$ eV]¹ combined with small $\sigma_a(\epsilon)$ values and possibly even Ramsauer-Townsend-type minima in $\sigma_a(\epsilon)$ for these gases at the low electron energies (such Ramsauer-Townsend minima have been observed for the nonfluorinated analogues¹³).

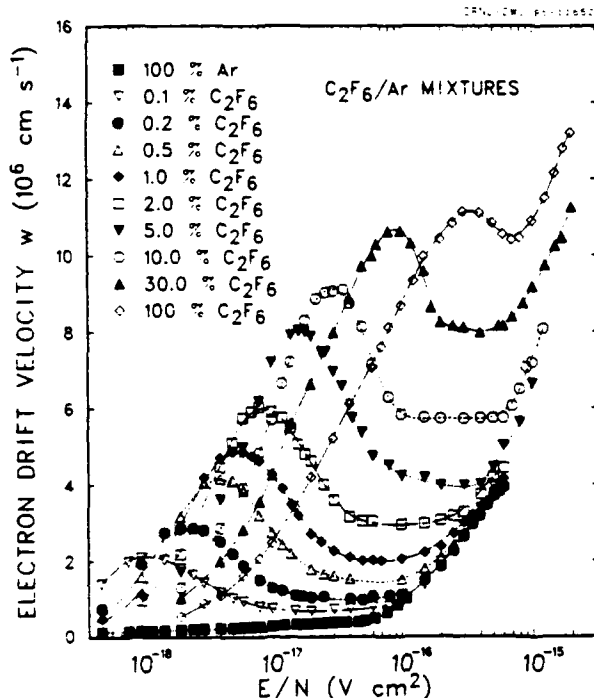


Fig. 2. Electron drift velocity w versus E/N for several C_2F_6 /Ar gas mixtures.

It is apparent from these figures that gas mixtures comprised of $>15\%$ of C_2F_6 in Ar possess peak w values of $>10^7$ cm s⁻¹, while at all concentrations of C_2F_6 in CH_4 , the peak value of w is 10^7 cm s⁻¹ or

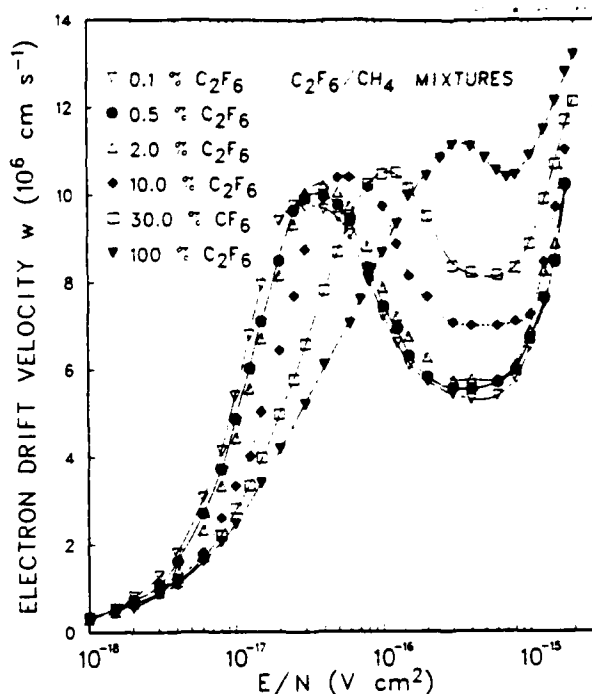


Fig. 3. Electron drift velocity w versus E/N for several C_2F_6 / CH_4 gas mixtures.

greater. Further it is evident from these findings that by varying the concentration of C_2F_6 in the buffer gas, the $w(E/N)$ functions can be chosen to have maximum values in the E/N range of $1-10 \times 10^{-17}$ V cm², which is roughly the range characteristic of the conduction stage of the switch (Fig. 1). The peak values of w in the C_2F_6 / CH_4 gas mixtures are considerably less sensitive to the fractional composition of the gas mixtures compared with the C_2F_6 /Ar gas mixtures.

Measurements of w in C_2F_6 / N_2 and C_2F_6 / CF_4 gas mixtures have also been made and are given in Figs. 4 and 5, respectively. Nitrogen has been used as a buffer gas in several small-scale switching experiments due primarily to the availability of a considerable electron swarm and electron beam cross section data base for this gas, making it amenable to theoretical modeling studies which may then be compared with experimental measurements.^{3,14-17} Switching experiments have recently been reported by Bletzinger in C_2F_6 / N_2 and C_3F_8 / N_2 gas mixtures.¹⁴ The w measurements given in Fig. 4 indicate that these gas mixtures are not particularly suited for switching applications as they do not show the pronounced electron drift velocity enhancement at low electric fields that the mixtures given in Figs. 2 and 3 possess.

Gas mixtures composed of varying percentages of C_2F_6 in CF_4 also do not show significant change in the drift velocity maximum (Fig. 5). Drift velocity measurements were made using this gas mixture to determine if the synergistic effects that we have observed on w in the C_2F_6 /Ar, C_2F_6 / CH_4 , and other attaching gas/ CH_4 and attaching gas/Ar gas mixtures (Figs. 2 and 3 and Ref. 1) would also be observed in this gas mixture. The measurements show that the electron drift velocity changes monotonically from that of pure CF_4 to that of pure C_2F_6 when the percentage of C_2F_6 is increased.

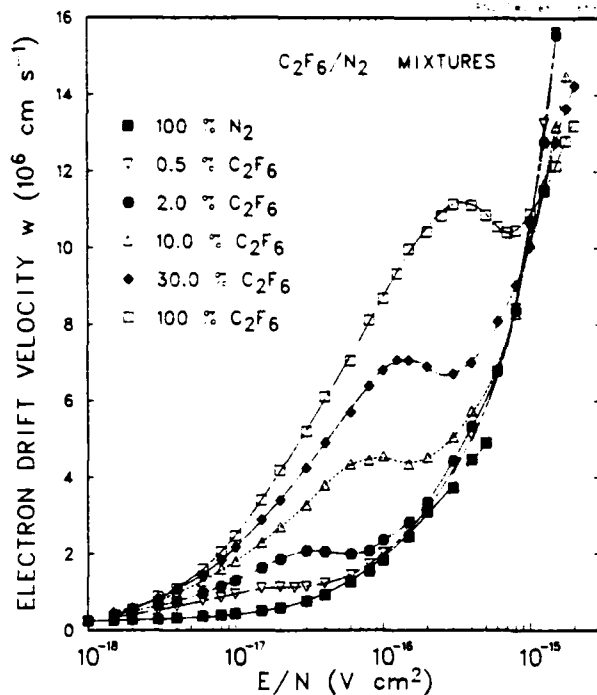


Fig. 4. Electron drift velocity w versus E/N for several C_2F_6/N_2 gas mixtures.

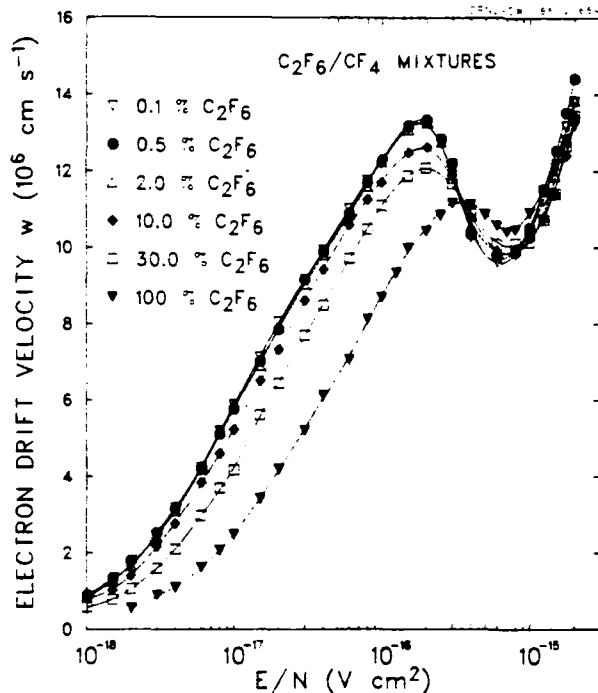


Fig. 5. Electron drift velocity w versus E/N for several C_2F_6/CF_4 gas mixtures.

Measurements of the attachment coefficient η/N normalized to the attaching gas number density N , and the effective ionization coefficient $(\alpha + \eta)/pN_T$ (where p is the fractional concentration of the attaching gas in the buffer gas and N_T is the total gas number density) in C_2F_6/Ar and C_2F_6/CH_4 gas

mixtures, obtained using the technique outlined in Ref. 18 are given in Figs. 6 and 7, respectively

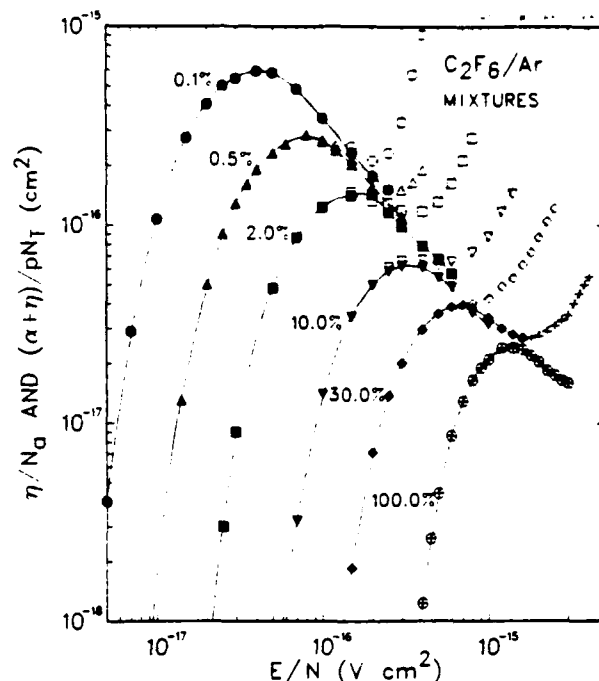


Fig. 6. The electron attachment coefficient η/N for C_2F_6 and the effective ionization coefficient $(\alpha + \eta)/pN_T$ (where p is the fractional concentration of C_2F_6 in the gas mixture) for the gas mixtures C_2F_6/Ar . The actual parameter measured in the electron attachment experiment is $(\alpha + \eta)$ (in units of cm^{-1}). This measurement can be either normalized to the attaching gas number density N , when $\alpha = 0$ to obtain the normalized attachment coefficient of the attaching gas constituent of the mixture (shown in the figure by the solid lines for various percentages of C_2F_6 in Ar), or it can be normalized to pN_T to find the effective ionization coefficient of the mixture as a whole (shown in the figure by the broken lines for various percentages of C_2F_6 in Ar).

When Ar is used as the buffer gas, the magnitude of the electron drift velocity and attachment coefficient and the positions of the maxima of these quantities when plotted as a function of E/N are very sensitive functions of the percentage of the attaching gas in the buffer gas. The peak positions move to higher E/N values and the magnitude of the attachment coefficient decreases by over one order of magnitude in going from 0.1 to 100% of the C_2F_6 (Fig. 6). Similar changes are observed for w in these mixtures, except that w increases with increasing concentration of the attaching gas (Fig. 2). The reason for this is that the addition of even small amounts of a molecular gas to argon drastically shifts the electron energy distribution function of the mixture to lower energies lowering the mean electron energy $\langle \epsilon \rangle$ and, consequently, increasing the E/N value which corresponds to the $\langle \epsilon \rangle$ value for which w and η/N maximize. In contrast to the measurements in argon, the attachment coefficient and electron drift velocity in the attaching gas methane gas mixtures are not nearly as sensitive to the attaching gas concentration as are the argon mixtures, particularly at low attaching gas concentrations. The addition of small amounts of a molecular gas to CH_4 has only a small influence on the

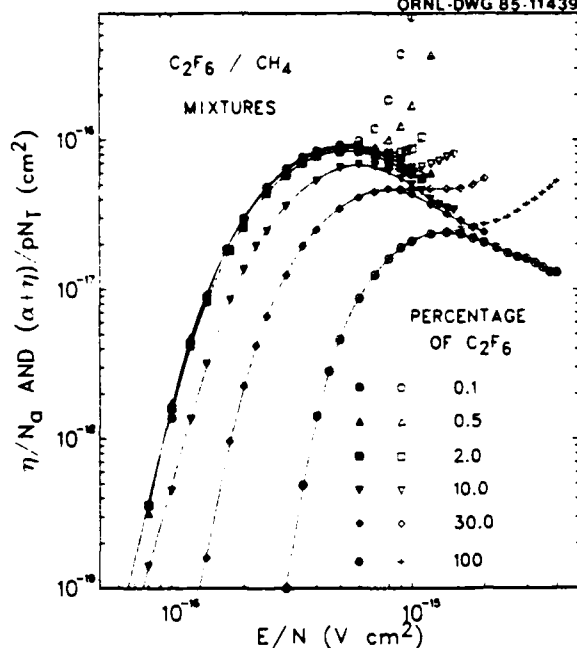


Fig. 7. The electron attachment coefficient η/N_a and effective ionization coefficient $(\alpha + \eta)/pN_T$ for C_2F_6/CH_4 gas mixtures. See Fig. 6 for an explanation of the symbols.

$w(E/N)$ and $\eta/N(E/N)$ for the mixture as CH_4 itself already possesses sizeable inelastic loss processes at low electron energies, and, consequently, the electron energy distribution function in the methane mixtures is only slightly modified.

These effects can be seen more clearly in Figs. 8 and 9, where $\eta/N(E/N)$ and $w(E/N)$ for selected gas mixtures of C_2F_6 in Ar and CH_4 buffer gases are plotted. These measurements indicate that the peak in η/N_a and w can be positioned at appropriate E/N values by either varying the attaching gas/buffer gas combination or by varying the percentage of the attaching gas in the buffer gas, so as to maximize the conductivity of the discharge when the switch is closed and also maximize the rate of decrease in the conductivity of the discharge and thus minimize the opening time of the switch when the switch is opened. The ability to tailor the gas mixture to position the maximum in w or η/N_a at given E/N values allows considerable freedom in designing the operating parameters of the diffuse discharge switch.

Measurements of $k_a(\langle E \rangle)$, $\eta/N_a(E/N)$, and $\alpha/N_a(E/N)$ at Elevated Gas Temperatures

The electron attachment rate constant $k_a(\langle E \rangle)$ has been measured for C_2F_6 over the temperature range $300 \leq T \leq 750$ K in order to investigate the influence of gas heating on the electron attaching properties of this molecule (Fig. 10).¹⁹ As the gas temperature increases, $k_a(\langle E \rangle)$ increases, and this increase is progressively larger at lower energies such that the threshold and the peak in the $k_a(\langle E \rangle)$ shift to lower energies at higher gas temperatures. The $k_a(\langle E \rangle)$ increases by $\approx 30\%$ over this temperature range near its peak at $\langle E \rangle \approx 3$ eV (Fig. 10).

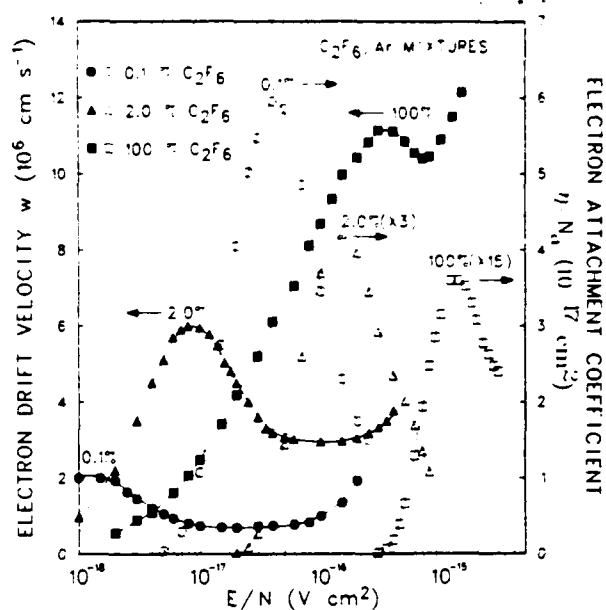


Fig. 8. Comparison of the electron attachment coefficient η/N_a and drift velocity w for C_2F_6 in selected gas mixtures of C_2F_6/Ar . The mixtures shown in this figure exhibit the desirable enhancement of the electron drift velocity at low E/N values and large electron attachment coefficients at high E/N values similar to the optimum characteristics displayed in Fig. 1.

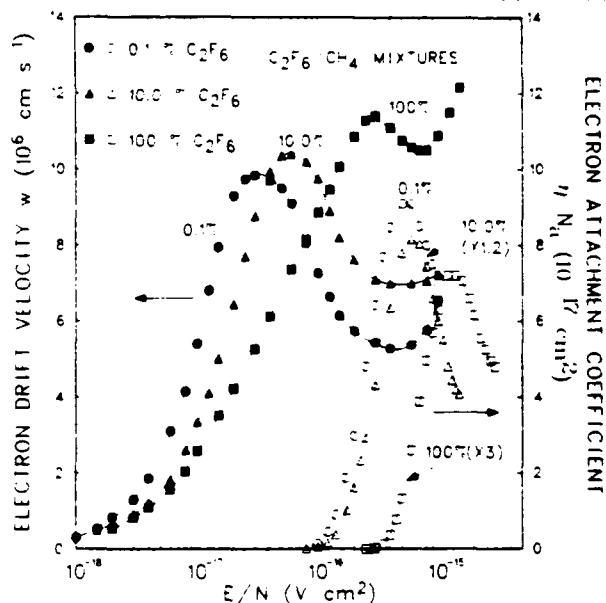


Fig. 9. Comparison of the electron attachment coefficient η/N_a and drift velocity w for C_2F_6 in selected gas mixtures of C_2F_6/CH_4 .

Additionally, we have measured the electron attachment coefficient η/N_a and the ionization coefficient α/N_a in pure C_2F_6 and in gas mixtures containing varying percentages of C_2F_6 in Ar at a gas temperature of 500 K in order to understand the influence of elevated gas temperatures on the trans-

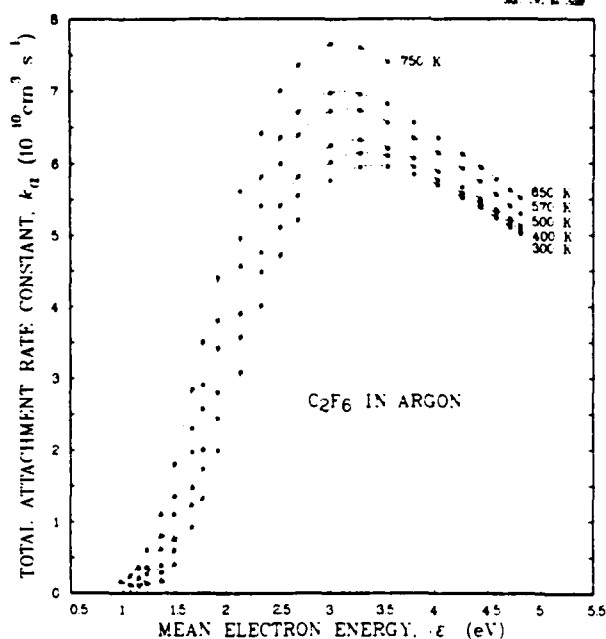


Fig. 10. Total electron attachment rate constant k_a as a function of the mean electron energy E for C_2F_6 at temperatures 300, 400, 500, 570, 650, and 750 K (from Ref. 19).

port and rate coefficients of gas mixtures for practical switching devices. These measurements, along with those obtained at room temperature (300 K) are given in Figs. 11 and 12. It is apparent from the measurements given in Fig. 11 that over the temperature range $300 \leq T \leq 500$ K the ionization coefficient is practically unchanged [to within the uncertainty of the present measurements ($\approx \pm 10\%$)] by increases in the gas temperature. The electron attachment coefficient in contrast increases considerably (by $\approx 25\%$) at higher E/N values with a much smaller increase in η/N occurring at E/N values close to the threshold for the attachment process ($E/N \approx 3 \times 10^{-16}$ V cm 2). The percentage increase in the rate of electron attachment to C_2F_6 in both the rate constant [$k_a(E/N)$] and the attachment coefficient [$\eta/N(E/N)$] studies (Figs. 10 and 11) near the peak in the attachment process are similar (being $\approx 10\%$ increase at 500 K) but for the $k_a(E/N)$ measurements [where the percentage of C_2F_6 in the Ar buffer gas is negligibly small (< 1 part in 10^6)], the greatest increase in k_a occurs near the threshold, while for the η/N measurements in pure C_2F_6 , the greatest change occurs at the higher E/N values near the tail of the attachment coefficient. This behavior can be more clearly seen in Fig. 12 where the attachment coefficient obtained from the rate constant measurements for C_2F_6 , ($\eta/N_a = k_a/w$, where w is the electron drift velocity in Ar) is plotted along with the measurements obtained for varying concentrations of C_2F_6 in Ar. These measurements indicate that as the percentage of C_2F_6 in Ar is increased, the change in η/N_a at threshold decreases, while the percentage increase in the electron attachment at the high energy tail increases with increasing C_2F_6 concentration. This observation is believed to be the result of changes in the electron energy distribution function in the swarm measurements with increasing C_2F_6 concentration, rather than actual changes in the attachment processes to C_2F_6 .

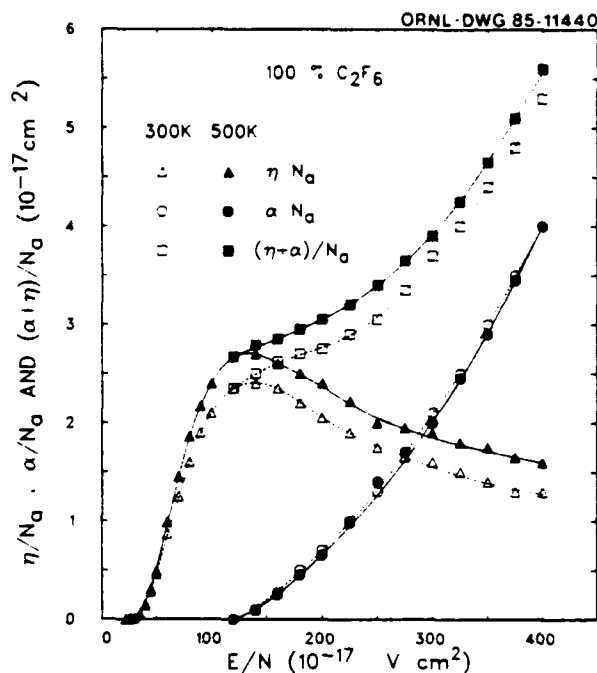


Fig. 11. Electron attachment coefficient η/N_a , electron ionization coefficient α/N_a and effective ionization coefficient $(\alpha + \eta)/N_a$ of pure C_2F_6 at 300 and 500 K as a function of E/N .

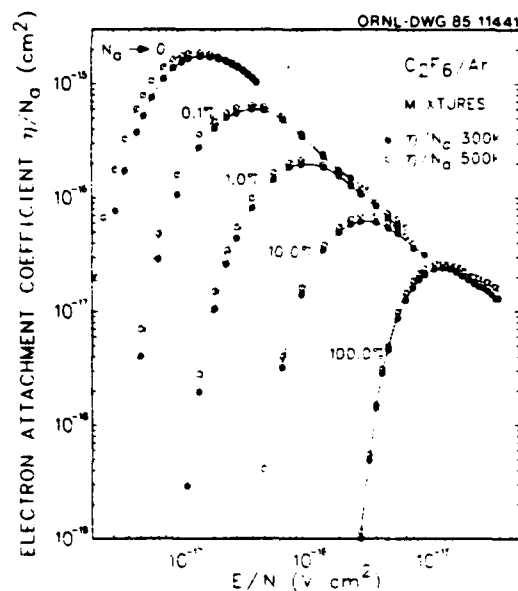


Fig. 12. Electron attachment coefficient η/N_a for several C_2F_6/Ar gas mixtures as a function of E/N . The measurements for $N_a = 0$ are obtained from the attachment rate constant measurements given in Fig. 10 where $\eta/N_a = k_a/w$ and N_a is very small (< 1 part in 10^6) compared with the buffer gas number density.

The influence of changes in the electron energy distribution function can also be seen in the drift velocity measurements for several C_2F_6/Ar gas mixtures given in Fig. 13. The greatest change in w occurs at the low E/N peak in the w curves for the C_2F_6/Ar mixtures, while the measurements at lower and higher E/N values appear to be unaltered by changes in gas temperature [to within the uncertainty of the measurements ($\approx \pm 5\%$)]. The drift velocity in pure C_2F_6 is considerably modified over the whole E/N range, and this may be the result of changes in the electron energy distribution function brought about by the increase in the electron attachment cross section at the higher gas temperatures. The influence that changes in the magnitude of the attachment coefficient have on the electron energy distribution function (and consequently upon the transport coefficients) has recently been discussed.²⁰ The changes in the electron drift velocity in the C_2F_6/Ar gas mixtures at elevated gas temperatures are expected to be considerably smaller than those in pure C_2F_6 , since the electron energy distribution functions in these mixtures are determined not only by the scattering processes in C_2F_6 but also by these processes in the more abundant Ar buffer gas, particularly at low C_2F_6 concentrations.

Measurements of k (cm^3/s) have also been performed in C_2F_6 as a function of gas temperature up to 750 K in Ar buffer gas (over the near electron energy range $0.76 \text{ eV} < \epsilon < 4.8 \text{ eV}$).²¹ These measurements are given in Figs. 14 and 15 and show that at a given value of ϵ , k decreases only slightly up to $T \sim 400 \text{ K}$, then rapidly decreases with increasing T up to $T \sim 450 \text{ K}$, and finally significantly increases with increasing T above this temperature. The lower temperature measurements ($T < 450 \text{ K}$) have been found to be strongly dependent on total gas pressure, indicating that parent negative ion formation processes are significant electron attachment processes at these temperatures.²¹ At higher gas temperature ($T \geq 450 \text{ K}$) pressure dependent electron attachment processes are negligible indicating that electron attachment to C_2F_6 at these temperatures is predominantly dissociative.²¹ The relative contributions of parent anion formation and dissociative attachment to the total electron attachment rate constant in C_2F_6 at a fixed value of ϵ as a function of gas temperature are given in Fig. 15. These measurements indicate that relatively small changes in the gas kinetic energy (and hence in the vibrational populations of the attaching gas) can have a large influence on the electron attaching properties of C_2F_6 which could, in turn, significantly affect the performance of repetitively operated switches operating at elevated gas temperatures using C_2F_6 .

Conclusions

The C_2F_6 /buffer gas mixtures discussed in this paper along with those mentioned in Ref. 1 are considered to be good candidates for diffuse discharge switching applications. These gas mixtures possess the desirable electron attachment and drift velocity characteristics displayed in Fig. 1 which are required to enhance the electron conduction when the switch is closed and then reduce the electron conduction as rapidly as possible when the switch is opened. These and other studies we have performed^{1,2,7,8,11-14} indicate that several of these gas mixtures have the further desirable characteristics of possessing relatively high breakdown field strengths [$(E/N)_{\text{brk}} > 10^{-15} \text{ V cm}^2$], good stability and low impurity product formation characteristics at room temperature which are desirable for diffuse discharge switches.

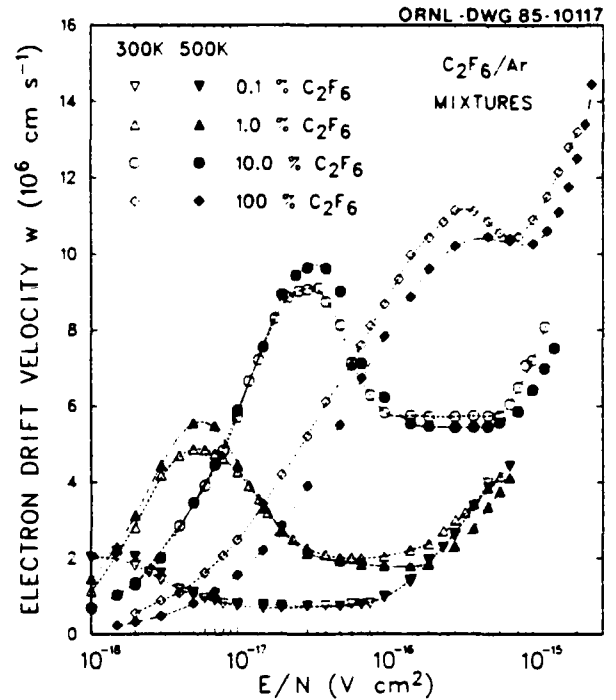


Fig. 13. Electron drift velocities as a function of E/N for several concentrations of C_2F_6 in Ar at gas temperatures of 300 and 500 K.

The increase in the rate of electron attachment that has been observed in C_2F_6 gas mixtures at the higher gas temperatures (Fig. 12) is not expected to seriously alter the characteristics of the diffuse discharge and may, in fact, be beneficial to the operation of the switch at these temperatures. On the other hand, the changes in the rate of electron attachment and the type of electron attachment processes (i.e., either parent anion formation or dissociative attachment) are significantly affected by the gas temperature in C_2F_6 (Fig. 15) and may significantly modify the response characteristics of a repetitively operated diffuse discharge switch at elevated gas temperatures. Further studies are needed to explore the influence of gas temperature on the breakdown strength and switching characteristics of these and other gas mixtures for possible use in diffuse discharge switches.

References

1. S. R. Hunter, J. G. Carter, and L. G. Christophorou, *Journal of Applied Physics* (submitted); L. G. Christophorou and S. R. Hunter, in *Electron-Molecule Interactions and Their Applications* (Academic Press, Orlando, Florida, 1984), Vol. 2, Chapt. 5.
2. K. Nakanishi, L. G. Christophorou, J. G. Carter and S. R. Hunter, *Journal of Applied Physics* (in press).
3. H. Harges, K. H. Schoenbach, G. Schaefer, H. Krompholz, and M. Kristiansen, in *Proceedings of the 4th IEEE Pulsed Power Conference* (The Texas Tech University Press, Lubbock, Texas, 1983), p. 474.
4. W. W. Byszewski, M. J. Enright, and J. M. Proud presented at the 4th IEEE Pulsed Power Conference, Albuquerque, New Mexico, June 6-8, 1983.

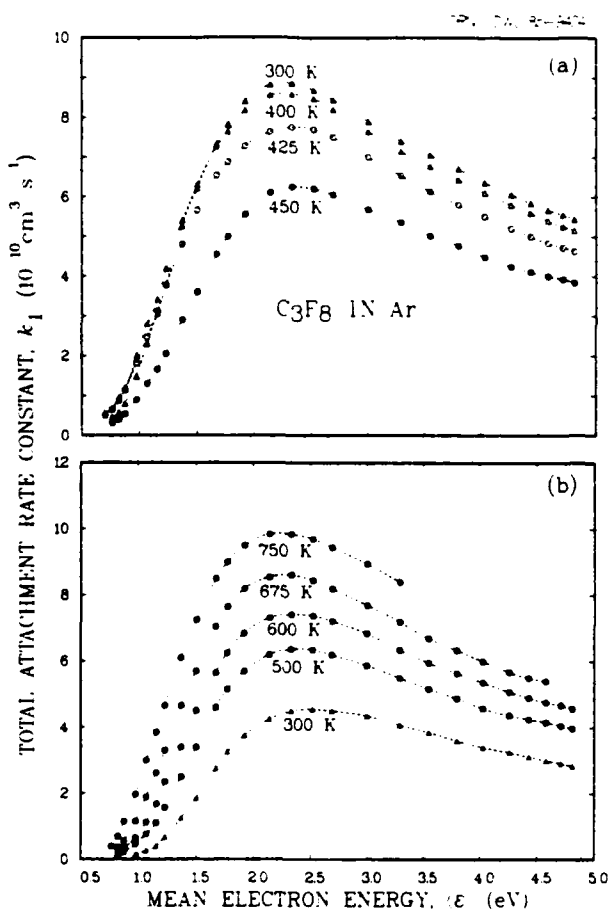


Fig. 14. Electron attachment rate constant k_1 for $N_2 \rightarrow \infty$ (and $N_2 = 0$) for C_3F_8 as function of mean electron energy $\langle \epsilon \rangle$ in a buffer gas of Ar at the gas temperatures given in the figure. The curve at 300 K in Fig. 14b is the dissociative attachment component to the total rate of electron attachment at this temperature (from Ref. 21).

5. L. C. Pitchford, private communication (1984).
6. R. N. DeWitt, in *Proceedings of the 4th IEEE Pulsed Power Conference* (The Texas Tech University Press, Lubbock, Texas, 1983), p. 223.
7. K. Nakanishi, L. G. Christophorou, J. G. Carter, and S. R. Hunter, this conference.
8. I. Sauers, W. D. Evans, and L. G. Christophorou, this conference.
9. K. H. Schoenbach, G. Schaefer, M. Kristiansen, L. L. Hatfield, and A. H. Guenther, *IEEE Trans. Plasma Sci.* **PS-10**, 246 (1982).
10. G. Schaefer, K. H. Schoenbach, A. H. Guenther, and W. K. Pendleton, in *Proceedings of the 4th IEEE Pulsed Power Conference* (The Texas Tech University Press, Lubbock, Texas, 1983), p. 602.
11. L. G. Christophorou, S. R. Hunter, J. G. Carter, and R. A. Mathis, *Appl. Phys. Lett.* **41**, 147 (1982).
12. L. G. Christophorou, S. R. Hunter, J. G. Carter, and V. K. Lakdawala, in *Proceedings of the 4th IEEE Pulsed Power Conference* (The Texas Tech University Press, Lubbock, Texas, 1983), p. 702.

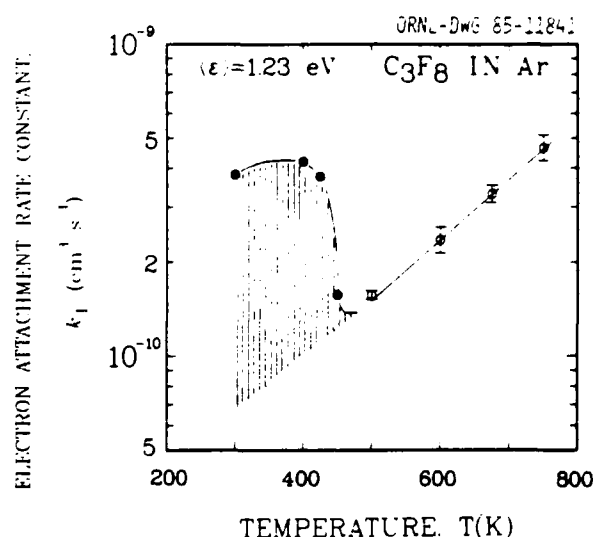


Fig. 15. Electron attachment rate constant k_1 for C_3F_8 versus temperature at a mean electron energy $\langle \epsilon \rangle = 1.23$ eV. The shaded area under the curve indicates the contribution of parent anion formation to the total rate of electron attachment (see Ref. 21).

13. D. L. McCorkle, L. G. Christophorou, D. V. Maxey, and J. G. Carter, *J. Phys. B* **11**, 3067 (1978).
14. P. Bletzinger, in *Proceedings of the 4th IEEE Pulsed Power Conference* (The Texas Tech University Press, Lubbock, Texas, 1983), p. 37.
15. V. E. Scherrer, R. J. Comisso, R. F. Fernsler, L. Miles, and I. M. Vitkovitsky, in *Gaseous Dielectrics III* (Pergamon Press, New York, 1983), p. 34.
16. V. E. Scherrer, R. J. Comisso, R. F. Fernsler, and I. M. Vitkovitsky, in *Gaseous Dielectrics IV* (Pergamon Press, New York, 1984), p. 238.
17. K. H. Schoenbach, G. Schaefer, M. Kristiansen, H. Kromholz, H. Harjes, and D. Skaggs, in *Gaseous Dielectrics IV* (Pergamon Press, New York, 1984), p. 246.
18. S. R. Hunter, J. G. Carter, and L. G. Christophorou, to be presented at the Joint Symposium on Swarm Studies and Inelastic Electron-Molecule Collisions, Tahoe City, California, July 19-23, 1985.
19. S. M. Spyrou and L. G. Christophorou, *J. Chem. Phys.* **82**, 2620 (1985).
20. H. A. Blevin, J. Fletcher, and S. R. Hunter, *Phys. Rev. A* **31**, 2215 (1985).
21. S. M. Spyrou and L. G. Christophorou, *Journal of Chemical Physics* (submitted).

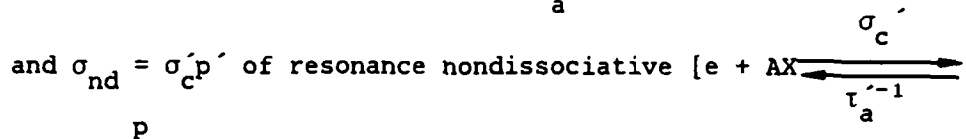
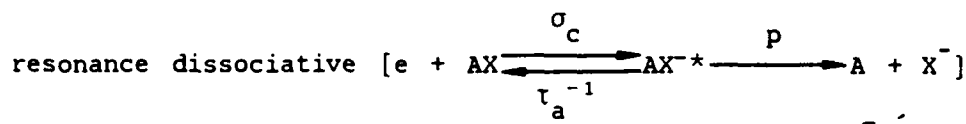
APPENDIX C

EFFECTS OF TEMPERATURE ON DISSOCIATIVE AND NONDISSOCIATIVE ELECTRON ATTACHMENT

L. G. Christophorou,* S. R. Hunter,
J. G. Carter, and S. M. Spyrou†

Atomic, Molecular and High Voltage Physics Group
Health and Safety Research Division
Oak Ridge National Laboratory
Oak Ridge, Tennessee 37831

Results of recent studies on the effects of temperature, T , on the dissociative and nondissociative electron attachment to molecules are presented and discussed. These show the delicate and large effects of T on the cross section $\sigma_{da} = \sigma_c p$ of



electron attachment to a molecule AX . For AX molecules where only dissociative attachment processes occur, the effect of T on σ_{da} is an increase in σ_{da} resulting from an increase in p principally because of a decrease in the separation time of A and X^{-} ; the energy integrated σ_{da} increases with increasing average internal energy of AX . For AX molecules with pure nondissociative attachment, the effect of T is a decrease of σ_{nd} with increasing T resulting from a decrease in p' (i.e., an increase with T of $\tau_a'^{-1}$). For AX molecules with both dissociative and nondissociative processes the total rate constant (or cross section) increases or

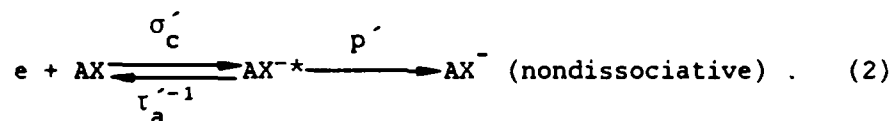
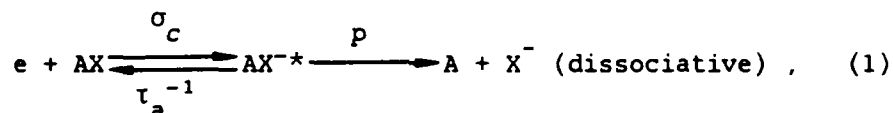
*Also, Department of Physics, The University of Tennessee, Knoxville, Tennessee 37996.

†Present address: Theoretical and Physical Chemistry Institute, The National Hellenic Research Foundation, 48, Vassileos Constantinou Avenue, Athens 501/1, Greece.

decreases with T depending on the relative contribution of the dissociative and nondissociative processes. It appears that for both dissociative and nondissociative attachment the effect of T on σ_c or σ'_c is small except in those cases where electron capture by the hot molecule is accompanied by geometrical changes. Besides their intrinsic value, these results are of applied significance in many areas where the operating temperatures are higher than ambient and where the number density of electrons and negative ions crucially affects the performance of the device.

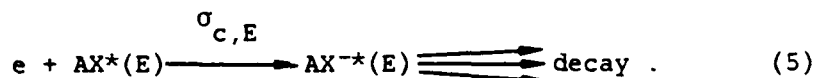
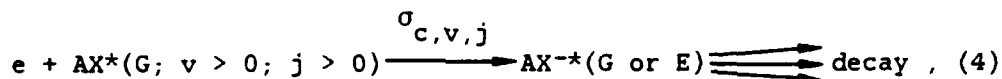
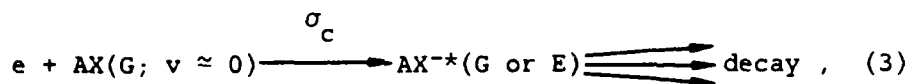
Introduction

Resonance electron attachment processes occur at low (<20 eV) energies and are generally discussed within the formalism of the resonance scattering theory and the formation of transient negative ions. Thus, resonance dissociative and nondissociative electron attachment to a molecule AX is viewed as occurring in two steps: (a) capture of the electron by AX to form the transient anion AX^{-*} and (b) the subsequent decay or stabilization of AX^{-*} ; viz.,



In reactions (1) and (2), σ_c and σ'_c are the respective electron capture cross sections, p and p' are the probabilities for AX^{-*} to decay by stable fragment [Eq. (1)] or parent [Eq. (2)] anion formation, and τ_a^{-1} and $\tau_a'^{-1}$ are the respective constants for AX^{-*} to decay by autodetachment. While many negative ion states (NISs) are usually involved in process (1), only one NIS (the lowest) is usually involved in process (2) [process (2) also requires that the electron affinity of AX is positive (>0 eV)]. In certain cases reactions (1) and (2) can proceed concomitantly and be in competition.

Processes (1) and (2) can be classified [1,2] according to the internal state of excitation of AX , viz.



In reaction (3), $AX(G = 0, v = 0)$ is a molecule in its ground electronic state G and predominantly in its lowest ($v = 0$) vibrational state of excitation, and $AX^{*-}(G \text{ or } E)$ is the transient anion formed in either the field of the ground (G) or the field of an excited (E) electronic state with a capture cross section σ_c . In reaction (4), $AX^*(G = 0, v > 0, j > 0)$ is a molecule in its ground electronic state, but in higher vibrational (v)/rotational (j) states, and $AX^{*-}(G \text{ or } E)$ is the respective transient anion formed with a cross section $\sigma_{c,v,j}$. In reaction (5) the target molecule $AX^*(E)$ is electronically excited, and the electron is captured in the field of an excited electronic state producing $AX^{*-}(E)$ with a cross section $\sigma_{c,E}$. Most studies to date concerned themselves with reaction (3). Swarm studies on reaction (5) are in progress at our laboratory. Electron attachment to "hot" molecules [reaction (4)] (the vibrationally/rotationally excited molecules can be formed by either laser excitation or by gas heating) have been reviewed [2].

In this paper we discuss reaction (4) with reference to published data and with reference to new results obtained at our laboratory on polyatomic halogenated compounds. Studies of the effects of temperature on the various electron attachment processes are of both intrinsic and of applied significance. With regard to the latter, in many applied areas the operating temperatures are higher than ambient and the performance of the various devices is crucially affected by the number density of electrons and negative ions (such is the case, for example, in diffuse discharge switches) and thus by T . Our discussion of resonance electron attachment to hot molecules will be separated into three parts: (a) electron attachment to molecules where only dissociative attachment processes occur, (b) electron attachment to molecules where only nondissociative electron attachment takes place, and (c) electron attachment to molecules where both dissociative and nondissociative electron attachment processes occur over an energy range.

Effects of Temperature on Electron Attachment to
Molecules Where Only Dissociative Attachment Occurs

Diatomic Molecules

The cross section, σ_{da} , for (1) can be expressed as

$$\sigma_{da} = \sigma_c p. \quad (6)$$

In Eq. (6) the capture cross section σ_c depends [2-4] on the autodetachment width Γ_a and the dissociation width Γ_d and varies inversely with the resonance energy ϵ_{max} ; the probability p is usually expressed as [2-4]

$$p = e^{-\tau_s/\tau_a}, \quad (7)$$

where τ_s is the average separation time of A and X^- , and τ_a is the average lifetime of AX^{*-} . As T increases, higher-lying vibrational levels of AX are populated for which the internuclear distances increase significantly (and hence the Franck-Condon region is broadened), and the magnitude of σ_{da} for molecules, AX^{*vibr} , in such excited nuclear motion states increases significantly; also, the threshold energy is lowered, and the Γ_d is increased (e.g., see Refs. 2, 5). Such an enhancement in σ_{da} , however, can be small in cases where the dissociative attachment process is exoergic and the potential energy curve for the transient negative ion AX^{*-} crosses that of the neutral molecule close to the equilibrium separation.

The increase in σ_{da} with T results from an increase in both σ_c [as higher vibrational levels of AX are populated, progressively lower energy electrons, for which σ_c is larger [2,6], are captured (also the Franck-Condon factors change)] and p . However, the increase in σ_c is usually small [except perhaps in those cases (e.g., N_2O [7]) where geometrical changes concomitant with electron capture occur] compared with that in p ; the latter dominates the T dependence of σ_{da} and results from a shortening of τ_s associated with the spatially more extended wavefunctions of AX^{*vibr} . Theoretical calculations [2,5,8,9] have shown that the effect of rotational excitation on σ_{da} is usually small and that the effect of vibrational excitation substantially accounts for the observed increases in σ_{da} with T.

The aforementioned conclusions are based on experimental and theoretical results on diatomic molecules (O_2 , H_2 , D_2 , HCl , DCl) [2,5,8-11]. Examples of these findings are shown in

Figs. 1 and 2. In Fig. 1 are plotted the calculated [8] values of σ_{da} close to the vertical onset for H/H_2 and D/D_2 for H_2 and D_2 in various vibrational levels v . In Fig. 2 the experimental (see figure caption) σ_{da} for Cl^- from HCl and DCl are shown for HCl/DCl in the $v = 0, 1$, and 2 levels. The σ_{da} increases dramatically as the vibrational quantum number increases. For a given pair of isotopic molecules, the lower the vibrational energy $h\nu_x$ of a given mode x is, the larger is the effect of T on σ_{da} since at a fixed T higher levels v_x are populated for which τ_s is shorter (p larger). It should be realized, however, that unless T is very large or ϵ_{max} small, the increase of the measured σ_{da} with T is much smaller than indicated in Figs. 1 and 2 because σ_{da} is the Boltzmann-factor-weighted σ_{da} for all levels v_x , and only a small fraction (itself a function of the size of $h\nu_x$) of molecules are in higher vibrational levels.

It has recently been pointed out [10] that the data in Figs. 1 and 2 show that the isotope effects observed [2,6] in the σ_{da} for H_2/D_2 and HCl/DCl (and for other molecules [2,6]) depend on T . As T increases, τ_s decreases and hence the isotope effects become less pronounced; for a given T , higher vibrational levels (for which p is larger) are populated in the heavier molecule ($h\nu_D < h\nu_H$) and thus the increase in σ_{da} with T is larger for the heavier than for the lighter analog (see insets in Figs. 1 and 2). Actually (see inset in Fig. 2), when HCl/DCl have vibrational energy >0.1 eV this increase in σ_{da} overtakes the opposite effect (decrease) introduced by the larger reduced mass of $D-Cl^-$ compared with $H-Cl^-$, so that the ratio $[\sigma_{da}(\epsilon_{max})]_{DCl}/[\sigma_{da}(\epsilon_{max})]_{HCl}$ which for HCl and DCl in the $v = 0$ level is equal to 0.71 (Ref. 12) becomes >1 .

The cross section data for the various v levels of H_2 and D_2 in Fig. 1 have been used [10] to determine the contributions to the total $\sigma_{da}(T)$ from the various vibrational levels at a number of T ; at each value of T the cross section for a particular vibrational level v (see Fig. 1) was multiplied by the fractional population of that level. The resultant cross sections $\sigma_{da}(v)$ are shown in Fig. 3 along with the total $\sigma_{da}(T)$ [the sum of $\sigma_{da}(v)$ over all contributing v levels]. Although these results are approximate (the cross sections in Fig. 1 for the various v are threshold values [8]), it is clear that as T increases the isotope effect decreases (see inset in Fig. 3).

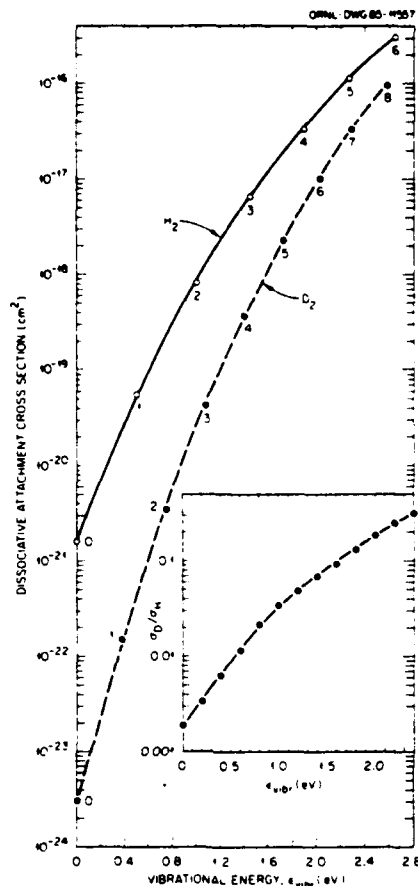


Figure 1. Calculated [8] σ_{da} for H^-/H_2 and D^-/D_2 with H_2/D_2 in various vibrational levels. The data are for energies close to the vertical onset. Inset: Ratio σ_D/σ_H of the σ_{da} for D^-/D_2 and H^-/H_2 as a function of the neutral molecule's vibrational energy (from Ref. 10).

Similar calculations [10] for HCl and DCl are more limited since for these molecules only cross section data for the $v = 0, 1$, and 2 levels are available (see Fig. 2) and the effect of rotational excitation of $\sigma_{da}(T)$ may not be insignificant [9,11] as was the case for H_2^{da} and D_2 [8,14]. Nevertheless, the contributions to the total dissociative attachment cross section $\sigma_{da}(T)$ from the $v = 0, 1$, and 2 vibrational levels in Fig. 4 show that the total $\sigma_{da}(T)$ of DCl exceeds that of HCl at $T > 650$ K (see inset in Fig. 4), while it is only 70% that of HCl at $T \approx 300$ K.

It is thus apparent [10] that the isotope effects observed in dissociative attachment depend on gas temperature; they are

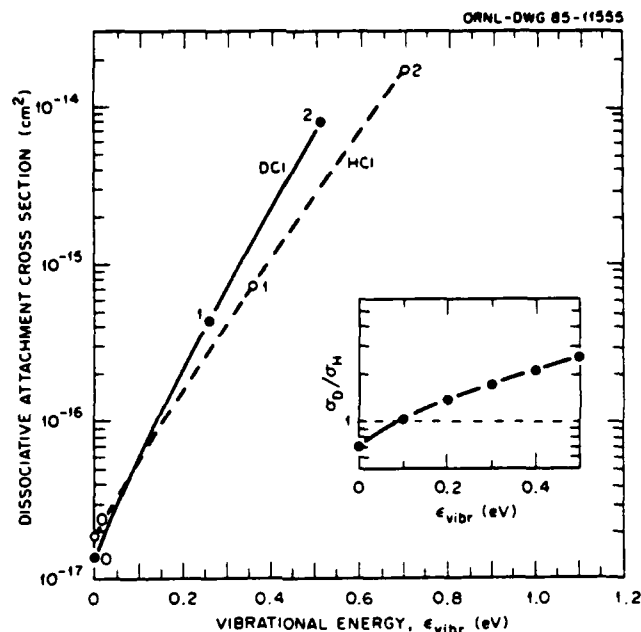


Figure 2. Experimental [11] σ_{da} for Cl^-/HCl and Cl^-/DCl for HCl and DCl in the $v = 0, 1$, and 2 levels. These cross sections were obtained from the values reported in Ref. 11 for the ratios $\sigma_{da}(v = 1, 2)/\sigma_{da}(v = 0)$ for HCl and DCl [$\sigma_{da}(v = 1)/\sigma_{da}(v = 0)$ and $\sigma_{da}(v = 2)/\sigma_{da}(v = 0)$ were reported [11] to be, respectively, 38 and 880 for HCl and 32 and 580 for DCl] and by normalizing the $\sigma_{da}(v = 0)$ relative cross section of Ref. 11 to the cross section measured [12] at $T \approx 300$ K (the peak value of σ_{da} for HCl and DCl is, respectively, equal to 1.95 and $1.4 \times 10^{-17} \text{ cm}^2$ at $\sim 0.8 \text{ eV}$ [12]) (from Ref. 10).

the largest when the isotopic molecules are in their $v = 0$ levels. It is also apparent that while for diatomic molecules the ratio $\sigma_{da}(v > 0)/\sigma_{da}(v = 0)$ increases with increasing vibrational energy, for a given T the internal energy is a function of the magnitude of $h\nu$, and for polyatomic molecules also of the number of vibrational degrees of freedom N .

Polyatomic Molecules

Earlier work on the effect of T on σ_{da} of polyatomic molecules has been reviewed [2]. Recent work on freons, which are of interest as additives in multicomponent gas mixtures for use as gaseous dielectrics or in diffuse discharge switches, has been undertaken at our laboratory, and some of the results we obtained are presented and discussed in this and the following sections.

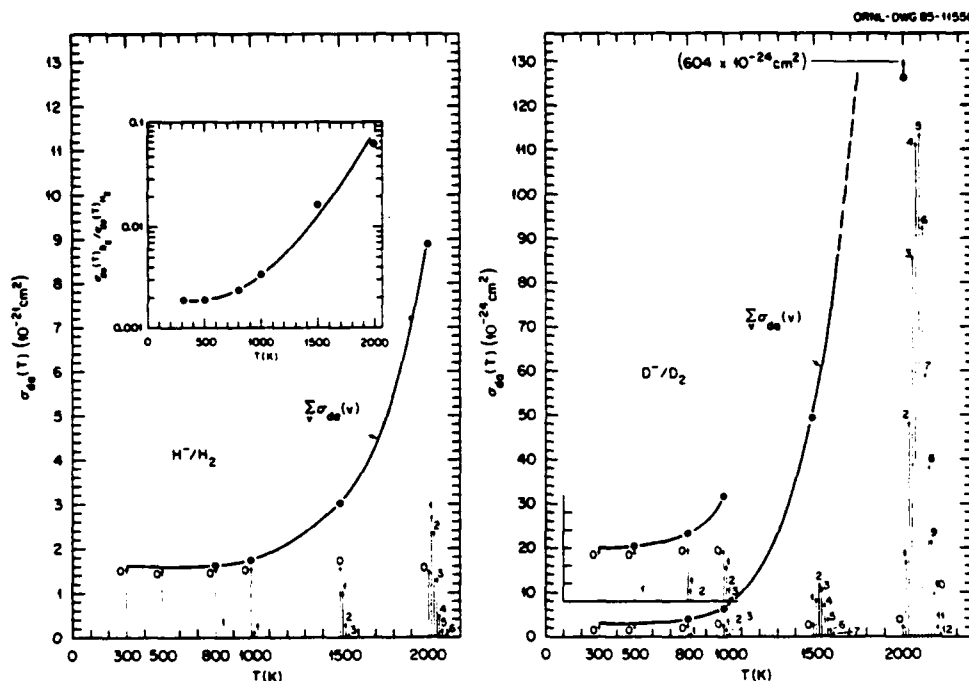


Figure 3. Dissociative attachment cross section $\sigma_{da}(T)$ for H^-/H_2 and D^-/D_2 at various T determined as described in the text. For each T the length of the vertical arrows designated by 0,1,2... gives the contribution $\sigma_{da}(v)$ to the total $\sigma_{da}(T) = \sum_v \sigma_{da}(v)$ of molecules, respectively, in the $v = 0,1,2...$ levels.

The energy, E_v , of the $v = 0,1,2...$ vibrational levels was determined using the formula $E_v = hc\omega(v + \frac{1}{2}) - hc\omega_e x_e(v + \frac{1}{2})^2$, where h is the Planck constant, c is the speed of light, and ω and $\omega_e x_e$ are the vibrational constants given in Ref. 13. As T increases, progressively larger contributions to $\sigma_{da}(T)$ come from molecules in higher vibrational quantum states. Inset: Ratio $\sigma_{da}(T)_{D_2} / \sigma_{da}(T)_{H_2}$ at various T (from Ref. 10).

CC2F₃. In Fig. 5 are given the measured [15] total electron attachment rate constants $k_a(\langle \epsilon \rangle)$ as a function of the mean electron energy $\langle \epsilon \rangle$ for $300 \leq T \leq 700$ K. As T increases, k_a increases, especially at low $\langle \epsilon \rangle$. In Fig. 6 are shown the total electron attachment cross sections $\sigma_a(\epsilon)$ obtained [15] at each value of T from the respective $k_a(\langle \epsilon \rangle, T)$ in Fig. 5 via the swarm unfolding technique [16]. The peak at ~ 1.5 eV is especially sensitive to changes in T . The peak value of $\sigma_a(\epsilon)$ is increased by a factor of 3, and the energy position, ϵ_{max} , of the peak and the energy onset, A_0 , shift progressively to lower energy as T increases. Electron beam studies (inset,

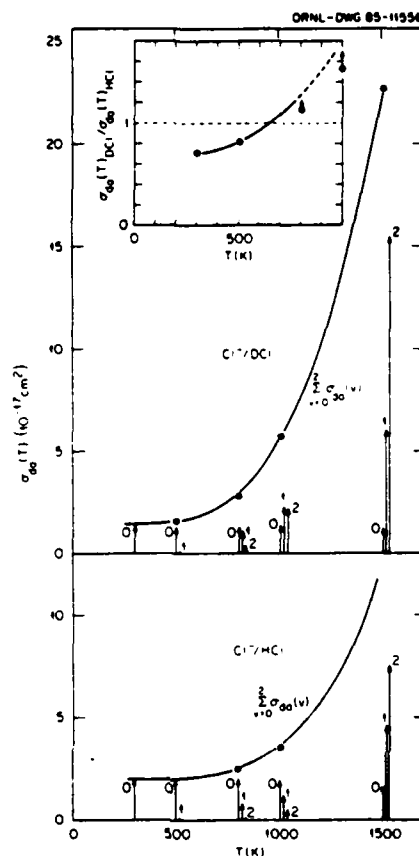


Figure 4. Dissociative attachment cross section $\sigma_{da}(T)$ for Cl_2/HCl and Cl_2/DCl at various T determined as described in the text. For each T the length of the vertical arrows designated by 0, 1, and 2 gives the contribution $\sigma_{da}(v)$ to the total $\sigma_{da}(T)$ of molecules, respectively, in the $v = 0, 1$, and 2 vibrational levels (the energy of each vibrational level was determined as described in the caption of Fig. 3). The sum, $\sum_{v=0}^2 \sigma_{da}(v)$, of the $\sigma_{da}(v)$ for the $v = 0, 1$, and 2 levels is also given in the figure. Since for $T \geq 1000$ K the contributions to $\sigma_{da}(T)$ of molecules in $v > 2$ is substantial, the values of $\sigma_{da}(T)$ [$\equiv \sum_{v=0}^2 \sigma_{da}(v)$] in the figure for 1000 and 1500 K are grossly underestimated. As a consequence of this, the values of the ratio $[\sigma_{da}(T)]_{\text{DCl}}/[\sigma_{da}(T)]_{\text{HCl}}$ for 1000 and 1500 K (see inset) are lower than their true values (this is indicated in the inset by the data points \bullet) (from Ref. 10).

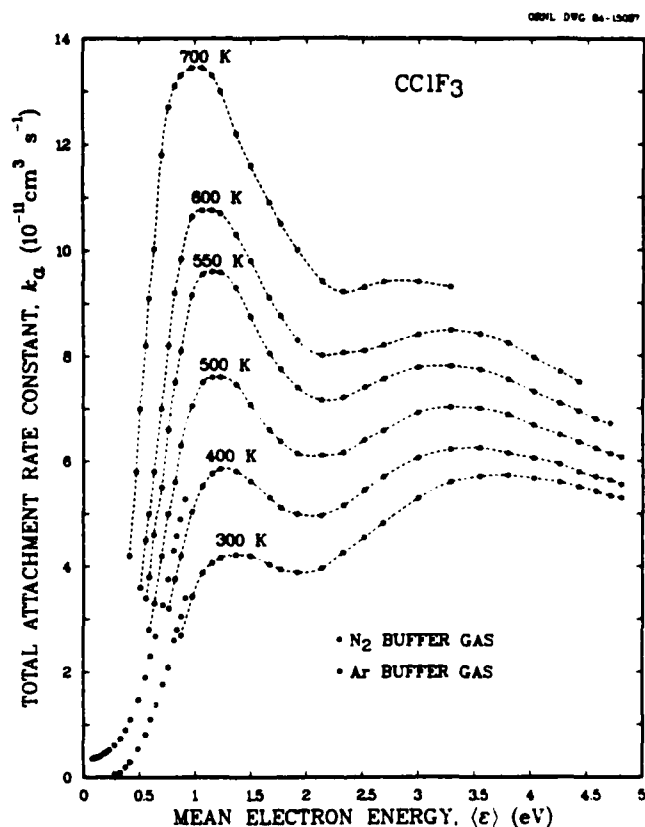


Figure 5. Total electron attachment cross section versus electron energy for CClF_3 measured [15] in the buffer gases N_2 or Ar at various temperatures; the $k_a(\langle \epsilon \rangle)$ were independent of gas number density.

Fig. 6) have shown [15] that at low gas pressures CClF_3 captures electrons exclusively via dissociative attachment and that the peaks at ~ 1.5 and ~ 4.7 eV are the former due to Cl^- and the latter due to Cl^- , F^- , CClF_2^- , and ClF^- ions.

C_2F_6 . In Fig. 7 the $k_a(\langle \epsilon \rangle, T)$ are given along with the relative abundance of the fragment negative ions observed (inset, Fig. 7) in a beam study [17]. No parent negative ions were observed in the low pressure beam study, and this is consistent with the absence of any pressure dependence of $k_a(\langle \epsilon \rangle, T)$ in the swarm study. In Fig. 8 are plotted the swarm unfolded cross sections which show a single peak due to F^- and CF_3^- (see inset of Fig. 7). The decrease in ϵ_{max} and AO and the increase in FWHM (full width at half maximum) of $\sigma_a(\epsilon)$ with T are shown in the inset of Fig. 8.

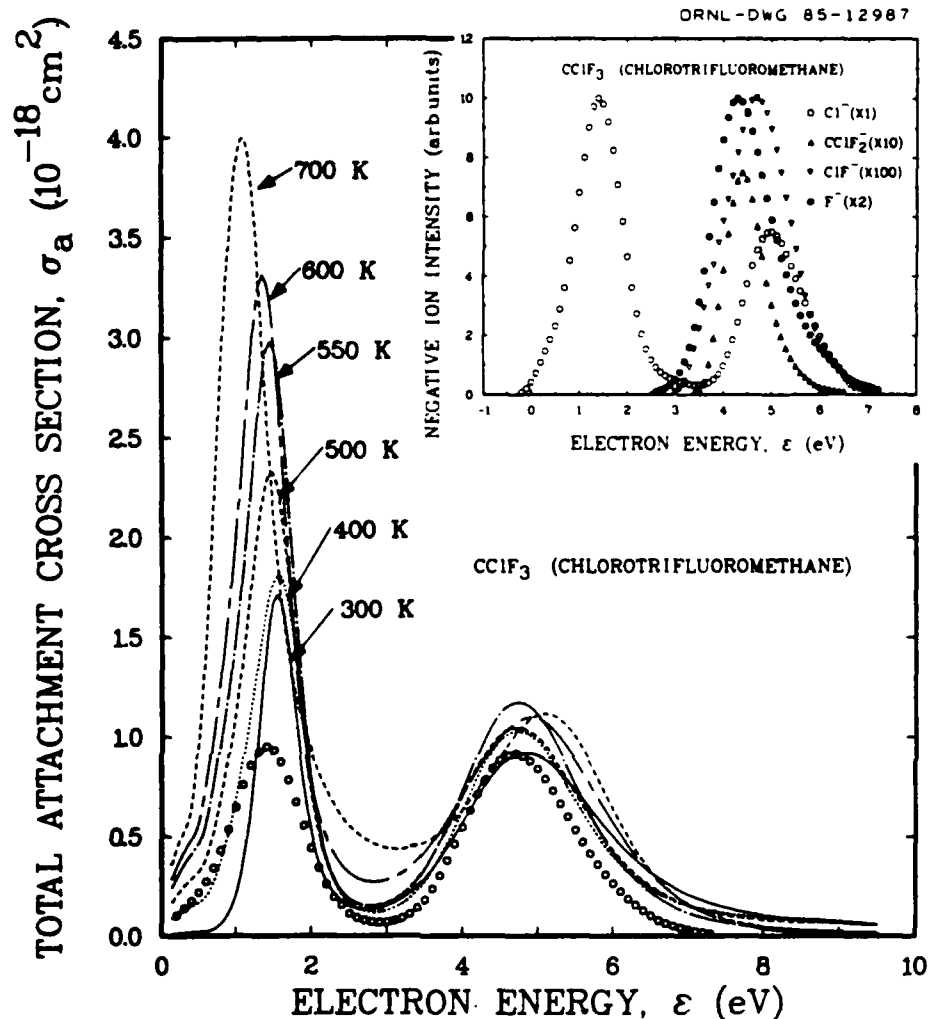


Figure 6. Total electron attachment cross section versus electron energy for CClF_3 unfolded from the $k_a(\langle\epsilon\rangle, T)$ data in Fig. 5 at various T . The curve designated by the open circles (o) is the electron beam total attachment cross section normalized to the high energy peak of the swarm unfolded cross section for 300 K. Inset: Relative intensity of the dissociative attachment negative ions produced by low energy electron impact on CClF_3 as a function of electron energy measured in a beam study (these spectra were corrected for the finite width of the electron pulse) [15].

In addition to the $k_a(\langle\epsilon\rangle, T)$ we measured in mixtures with Ar, we also measured the electron attachment, $\eta/N_a(E/N)$, and ionization, $\alpha/N_a(E/N)$, coefficients in pure C_2F_6 at 300 and

QRNL-DWG 85-12990

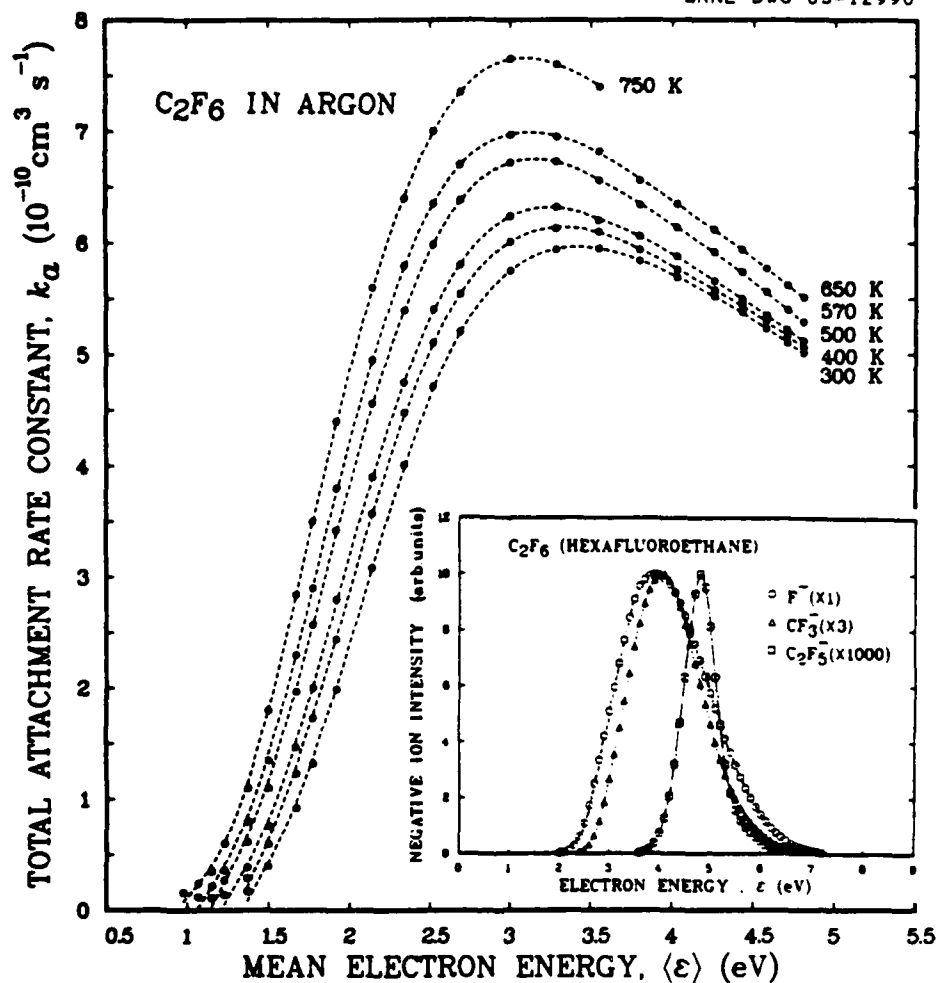


Figure 7. Total electron attachment rate constant as a function of mean electron energy for C₂F₆ in Ar buffer gas at various temperatures. The $k_a(\langle \epsilon \rangle, T)$ were independent of gas number density [15]. Inset:^a Relative intensity of the dissociative attachment fragment anions measured [17] in a low pressure beam study.

500 K. These measurements are shown in Fig. 9. The η/N_a data are consistent with those obtained in mixtures of C₂F₆ with Ar (Fig. 7).

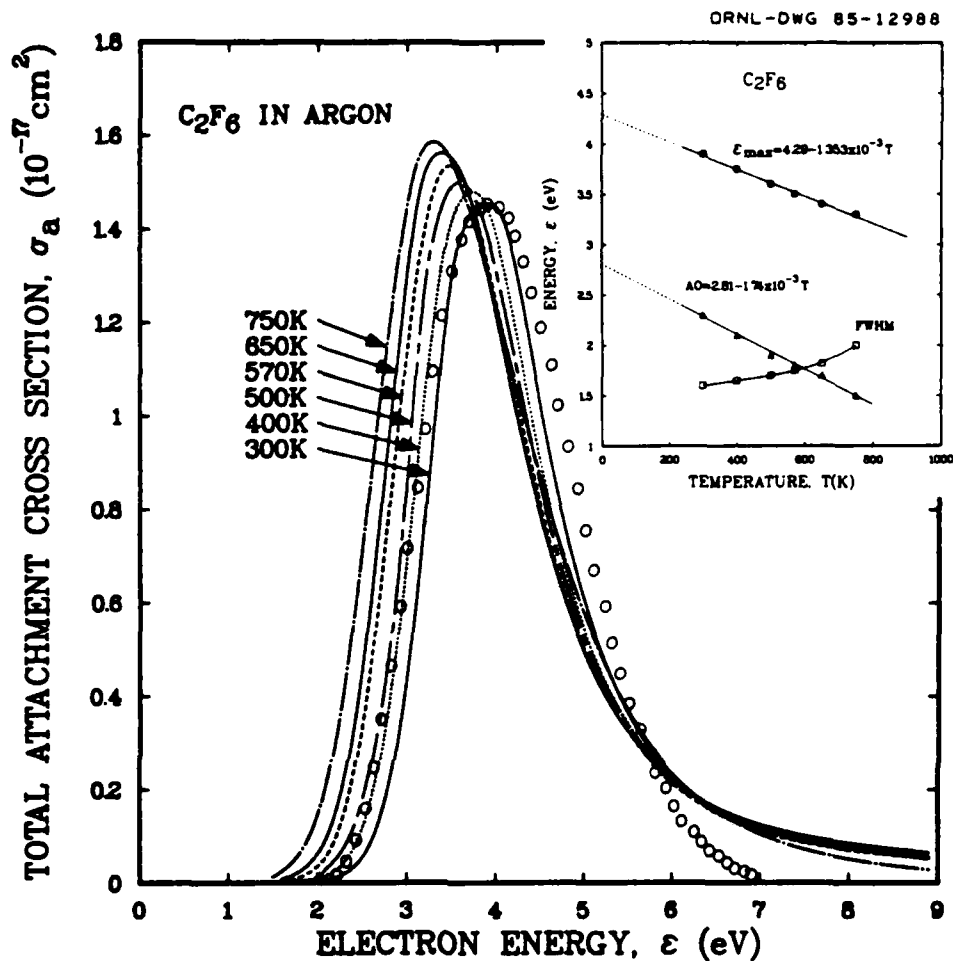


Figure 8. Total electron attachment cross section versus electron energy unfolded from the $k_a(\langle \epsilon \rangle, T)$ data in Fig. 7 at the indicated temperatures. The open circles (o) are the total electron beam cross section normalized to the peak of the swarm unfolded cross section for 300 K. Inset: Variation of the cross section peak position (ϵ_{max}), cross section onset energy (AO), and cross section full width at half maximum (FWHM) with temperature (from Ref. 15).

Variation of the Energy Integrated Attachment Cross Section with Temperature and with the Molecule's Internal Energy

We have determined the energy integrated attachment cross section

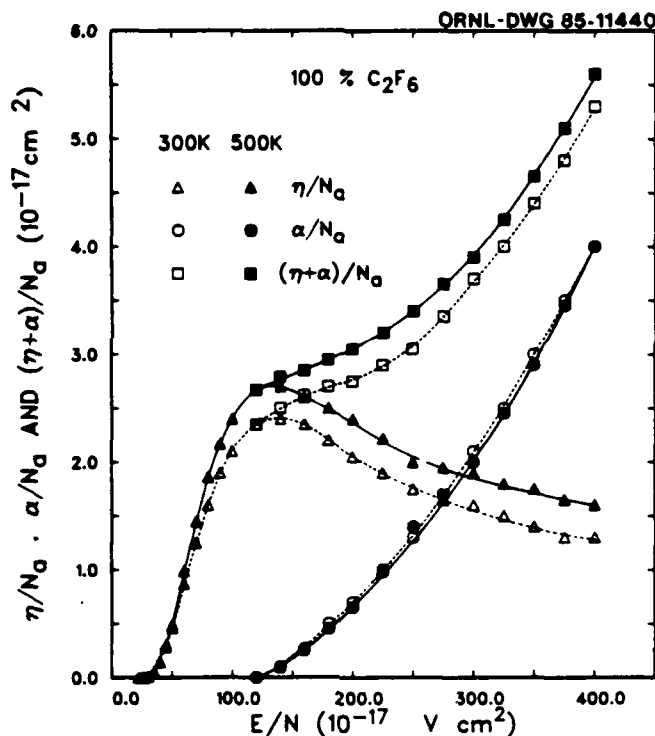


Figure 9. Electron attachment, η/N_a , and ionization, α/N_a , coefficients and their sum, $(\eta + \alpha)/N_a$, as a function of E/N at 300 and 500 K for pure C_2F_6 .

$$\int_{\epsilon_{\min}}^{\epsilon_{\max}} \sigma_{da}(\epsilon, T) d\epsilon \equiv \sigma_{EIA}(T) \quad (8)$$

from the respective $\sigma_{da}(\epsilon, T)$ measured for O^-/O_2 [18], Cl^-/HCl [11,19], $Cl^-/CClF_3$ [15], O^-/N_2O [7,20], SF_5^-/SF_6 [22,23], C_2F_6 [15] (all ions), and C_3F_8 [26] (all ions). These are plotted in Fig. 10a. The σ_{EIA} increases with T ; this increase varies from molecule to molecule but not, however, in the simple fashion (i.e., the lower the σ_{EIA} at $T = 300$ K the faster its increase with T) stated earlier [27].

The fast increase of σ_{EIA} with T for SF_5^-/SF_6 and O^-/N_2O is most interesting. For SF_6 this may be due to the larger increase in p with increasing T probably because almost all 15 vibrational frequencies of SF_6 are small [774 cm^{-1} (singly degenerate); 642 cm^{-1} (doubly degenerate); 948, 616, 525, and 347 cm^{-1} (all triply degenerate)] [28] and hence high-lying levels of each mode are populated at relatively low T ; also, it should be noted that the ϵ_{\max} for SF_5^-/SF_6 is low (~ 0.37 eV

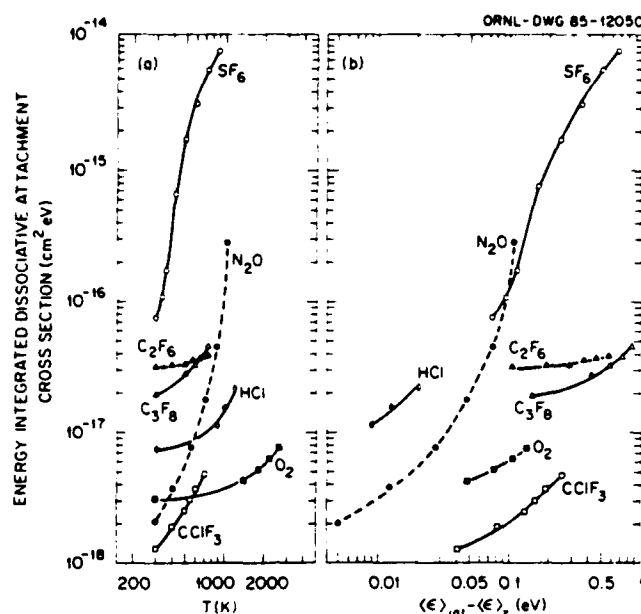


Figure 10. Energy integrated dissociative attachment cross section as a function of temperature (Fig. 10a) and excess internal energy $\langle \epsilon \rangle_{int} - \langle \epsilon \rangle_z$ (Fig. 10b) for O₂, HCl, N₂O, SF₆, CClF₃, C₂F₆, and C₃F₈ (see the text).

[24]) and that all six SF₅-F coordinates lead to SF₅⁻. For N₂O the large increase of σ_{EIA} with T may result from the fact that as T increases the hot N₂O* molecule (in the bending mode) [7,29] better facilitates upon electron collision the geometrical changes (from a straight N₂O* to a bend N₂O*-*) which are known to occur concomitantly with electron capture. It has been suggested [7] that the increased excitation in the bending mode of N₂O results in a lowering of the position of the NIS which leads to O⁻ formation; this would increase greatly the magnitude of σ_c and, thus, σ_{da} .

At any T there is a Boltzmann distribution B_v of the population of the vibrational levels v of each vibrational mode x. For a molecule with N normal modes, the vibrational energies of the normal mode x in the v = 0, 1, 2, ... levels (if we neglect anharmonicity) are $\epsilon_{v,x} = (v + \frac{1}{2})h\nu_x$ and for each x

$$B_v = e^{-\epsilon_{v,x}/kT} / \sum_{v=0}^{\infty} e^{-\epsilon_{v,x}/kT} \quad (9)$$

If we neglect the effect of rotational excitation and consider only the effect of vibrational excitation to be significant,

then for a diatomic molecule the cross section $\sigma_{da}(\epsilon, T)$ can be expressed as

$$\sigma_{da}(\epsilon, T) = \sum_{v=0}^{\infty} B_v \sigma_{da}^v(\epsilon, T) . \quad (10)$$

For a polyatomic molecule the summation in (10) must be carried out for all x . However, even if this were possible the x are not independent.

Let us then assume that as T increases each vibrational mode x of a polyatomic molecule is excited by an equal probability and that the total average internal energy $\langle \epsilon \rangle_{int}$ of the molecule is principally the sum of the energy in the various normal modes, x , viz.

$$\langle \epsilon \rangle_{int} = \sum_{x=1}^N \sum_{v=0}^{\infty} D_x B_v \epsilon_{v,x} , \quad (11)$$

where D_x is the degeneracy of the mode x . If we take $\langle \epsilon \rangle_{int}$ to be the molecule's total internal energy, then the molecule's excess energy would be $\langle \epsilon \rangle_{int} - \langle \epsilon \rangle_z$, where $\langle \epsilon \rangle_z$ ($\equiv \sum_{x=1}^N \frac{1}{2} h\nu_x$) is the zero-point energy. If now, $\langle \epsilon \rangle_{int} - \langle \epsilon \rangle_z$ is distributed quickly among the molecule's N vibrational degrees of freedom and can thus become available for the dissociative attachment reaction, one might expect a relationship between σ_{EIA} and $\langle \epsilon \rangle_{int} - \langle \epsilon \rangle_z$. Indeed, σ_{EIA} increases with $\langle \epsilon \rangle_{int} - \langle \epsilon \rangle_z$ (see Fig. 10b), although this increase differs--as expected--from one molecule to another. Actually, a better comparison might have been a plot of σ_{EIA} versus $(\langle \epsilon \rangle_{int} - \langle \epsilon \rangle_z) / \epsilon_{max}$. This would shift the C_2F_6 , C_3F_8 , O_2 , and $CClF_3$ curves to lower energies compared with SF_6 for which $\epsilon_{max} = 0.37$ eV. The fact that the curves in Fig. 10b for SF_6 and N_2O mesh reasonably well although ϵ_{max} for SF_6 is 0.37 eV and for N_2O it is 2.25 eV is consistent with the arguments presented earlier in this section that the ϵ_{max} for electron attachment to N_2O^* (bending mode) is lower than the ϵ_{max} for electron attachment to unexcited N_2O .

While further experimental and theoretical work is necessary (especially on polyatomic molecules) to fully understand the effect of temperature on $\sigma_{da}(\epsilon)$ and $\sigma_{EIA}(T)$, it is clear that for both diatomic and polyatomic molecules the changes in $k_{da}(\langle \epsilon \rangle)$, $\sigma_{da}(\epsilon)$, and $\sigma_{EIA}(T)$ with T result principally from an increase with T of the internal energy (\approx vibrational) of the molecule.

Effect of Temperature on Nondissociative Electron Attachment

The cross section, σ_{nd} , for nondissociative electron attachment--as that, σ_{da} , for dissociative varies profoundly with the gas temperature. Based on the data outlined in this section, this dependence arises from an effect of T on both σ'_c and p' . However, while for dissociative attachment σ_{da} generally increases with T , for nondissociative attachment σ_{nd} generally decreases with T . Furthermore, while in dissociative attachment the increase in σ_{da} with T is predominantly due to a decrease in τ (and thus increase in p), the decrease in σ_{nd} for nondissociative attachment is due to a decrease in τ_a (and thus decrease in p) and σ'_c . These conclusions are based on the following results.

SF₆

The cross section for the formation of SF₅⁻ from SF₆ at ~0.0 eV has been found to increase dramatically with increasing T (Fig. 10; Refs. 2, 22). However, a number of studies [2] have shown that the total attachment cross section or rate constant for SF₆ is independent of T to ~1200 K. This implies that the formation of SF₆⁻ (whose σ_{nd} peaks at ~0.0 eV [2]) decreases with increasing T . Direct evidence for this is provided by the early work of Hickam and Berg [30]. It is presently not possible to which quantity, σ'_c or p' , to ascribe this decrease in σ_{nd} with T , although p is expected to decrease with increasing T because τ_a is expected to decrease as the internal energy of SF₆^{-*} increases [2,6].

1-C₃F₆

A large decrease of the attachment rate constant for nondissociative electron attachment to perfluoropropylene (1-C₃F₆) with increasing T has been observed (Fig. 11; Refs. 2, 31, 32). This has been attributed [31,32] to a decrease in the τ_a of 1-C₃F₆^{-*} with increasing T .

C₆F₆

A profound decrease in the rate constant for electron attachment to perfluorobenzene (C₆F₆) with T has been reported for C₆F₆ (Fig. 12; Ref. 33). At $T = 300$ K, C₆F₆ forms parent C₆F₆⁻ ions by capturing near-zero energy electrons [2]; the τ_a of C₆F₆^{-*} was found to be ~10 μ s [2]. Spyrou and Christophorou [33] concluded that the decrease in $k_a(\langle \epsilon \rangle)$ with T (Fig. 12) cannot be attributed to a decrease in τ_a (decrease in p) with T [the $k_a(\langle \epsilon \rangle)$ did not depend on the gas number

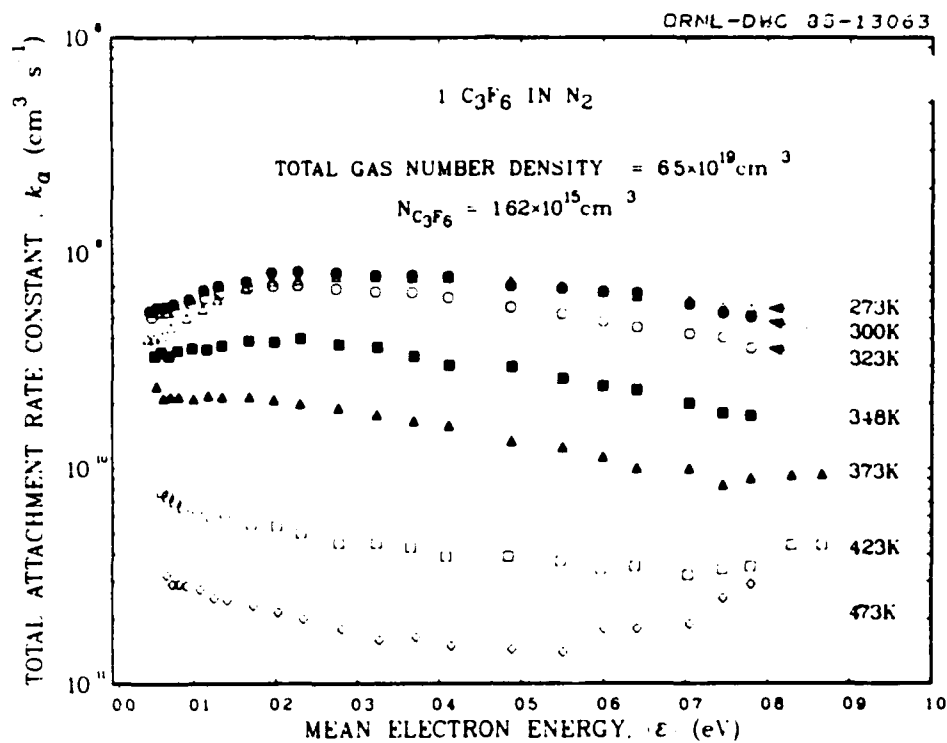


Figure 11. Total attachment rate constant versus mean electron energy for 1-C₃F₆ in N₂ at $273 \leq T \leq 473$ K (from Ref. 32).

density at any T] or other by-products resulting from gas heating. They attributed it to a decrease in σ'_c and suggested that the increase in the internal energy of C₆F₆ affects rather profoundly the rate for the capture transition (i.e., to differences in the magnitude of σ'_c for the reactions $e + \text{C}_6\text{F}_6 \rightarrow \text{C}_6\text{F}_6^{-*}$ and $e + \text{C}_6\text{F}_6^* \rightarrow \text{C}_6\text{F}_6^{-*}$).

While much improvement in our understanding of the effects of the internal energy of a molecule on its electron attachment properties is still desirable, it is clear that as a rule σ_{da} increases and σ_{nd} decreases with increasing internal energy, that is, increasing T. It is also apparent that for both dissociative and nondissociative electron attachment p is the determining factor unless geometrical changes concomitant with electron capture effect changes in σ_c or σ'_c .

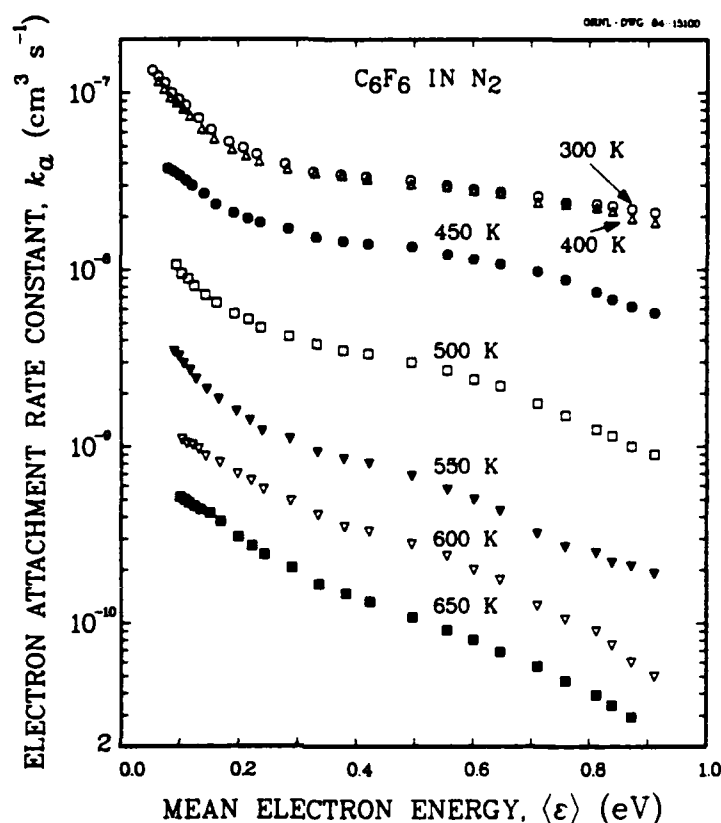


Figure 12. $k_a(\langle\epsilon\rangle, T)$ for C_6F_6 measured in a buffer gas of N_2 . The C_6F_6 gas number density varied from 0.41 to $46.3 \times 10^{13} \text{ cm}^{-3}$ and that of N_2 from 2.25 to $6.44 \times 10^{19} \text{ cm}^{-3}$ (from Ref. 33).

Effect of Temperature on the Measured Attachment Rate Constant and Cross Section for Molecules for Which Both Dissociative and Nondissociative Electron Attachment Occur Over an Energy Range

Recently, we measured [26] the total electron attachment rate constant $k_a(\langle\epsilon\rangle)$ for C_3F_8 in Ar in the temperature range from 300 to 750 K. At $T < 425$ K the $k_a(\langle\epsilon\rangle)$ were found to increase with increasing total gas number density N_t over the entire $\langle\epsilon\rangle$ range (~ 0.5 to ~ 5 eV) covered in these experiments. At 450 K, the $k_a(\langle\epsilon\rangle)$ increased with N_t only for $\langle\epsilon\rangle < 1.2$ eV and at $T > 450$ K the $k_a(\langle\epsilon\rangle)$ were independent of N_t . The $k_a(\langle\epsilon\rangle)$ also showed a weak dependence on the attaching gas number density N_a due to the effect of the presence of the attaching gas on the distribution functions of pure Ar used in

the analysis; this effect was taken into account by measuring, for a fixed N_t , the $k_a(\langle\epsilon\rangle)$ as a function of N_a and extrapolating at each $\langle\epsilon\rangle$ the $k_a(N_a)$ to $N_a \rightarrow 0$.

In Fig. 13 are plotted the values, $k_1(\langle\epsilon\rangle)$, of $k_a(\langle\epsilon\rangle)$ for $N_a \rightarrow 0$ and $N_t \rightarrow 0$ for all values of T that data were taken, and in Fig. 14 k_1 is plotted as a function of T for two values of $\langle\epsilon\rangle$. It is evident from these data that $k_1(\langle\epsilon\rangle)$ decreases to a minimum around 450 to 500 K and that it then increases as T increases.

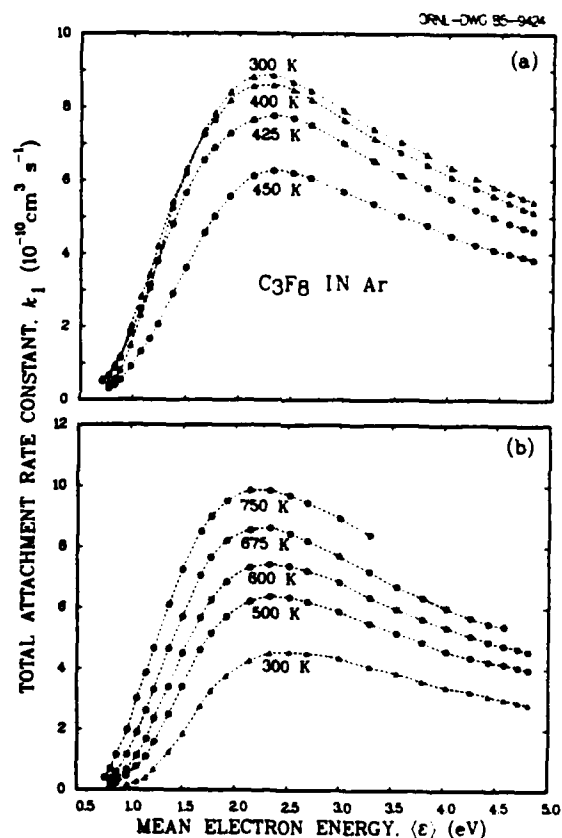


Figure 13. Electron attachment rate constant k_1 ($N_a \rightarrow 0$; $N_t \rightarrow \infty$) for C_3F_8 measured as a function of mean electron energy $\langle\epsilon\rangle$ in a buffer gas of Ar at (a) 300, 400, 425, and 450 K and (b) 500, 600, 675, and 750 K. The 300 K curve in Fig. 13b is the dissociative attachment contribution to the measured $k_a(\langle\epsilon\rangle)$ at this temperature (see the text and Ref. 26).

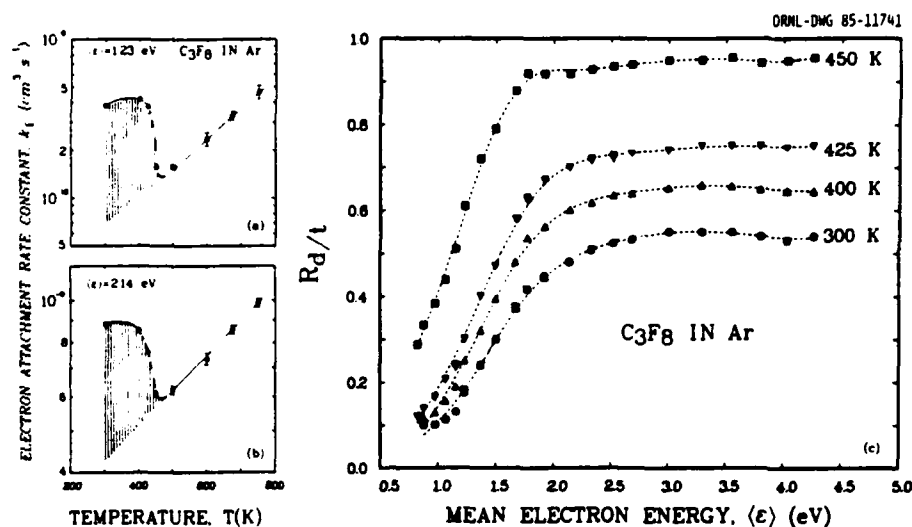


Figure 14. (a) and (b) Electron attachment rate constant k_1 ($N_a \rightarrow 0$; $N_t \rightarrow \infty$) for C_3F_8 versus temperature T at the mean electron energies $\langle \epsilon \rangle = 1.23$ and 2.14 eV. (c) Ratio R_d/t of the attachment rate constant due to dissociative attachment to the total attachment rate constant (see the text) versus the mean electron energy at 300, 400, 425, and 450 K obtained from extrapolation of the $k_a(\langle \epsilon \rangle)$ measured at $T \geq 500$ K to lower T (see the text).

The delicate dependence of $k(\langle \epsilon \rangle)$ on T can be understood by considering the results of electron beam and electron swarm studies. Single collision beam experiments on C_3F_8 indicated the presence of only dissociative attachment anions and established their identity and energy dependence; they also showed the existence of a number of NISs which lead to dissociative attachment [17]. On the other hand, the results of high pressure swarm experiments on C_3F_8 determined the magnitude of the total attachment rate constant and cross section as a function of electron energy and their total pressure dependence [26,34]; they indicated that in addition to the NISs which lead to dissociative attachment (observed in single collision beam experiments) there exists another, lower-lying NIS which is attractive and which leads to the formation of parent negative ions with $\tau_i < 10^{-6}$ s [26,34]. These findings and the observed effects^a of T on $k(\langle \epsilon \rangle)$ (Figs. 13 and 14) and $\sigma_{da}(\epsilon)$ (Fig. 15) have been ascribed^a to electron attachment via an attractive NIS (with a positive electron affinity and a steep repulsive part) leading to parent anions and to one (or more) repulsive NISs leading to fragment anions.

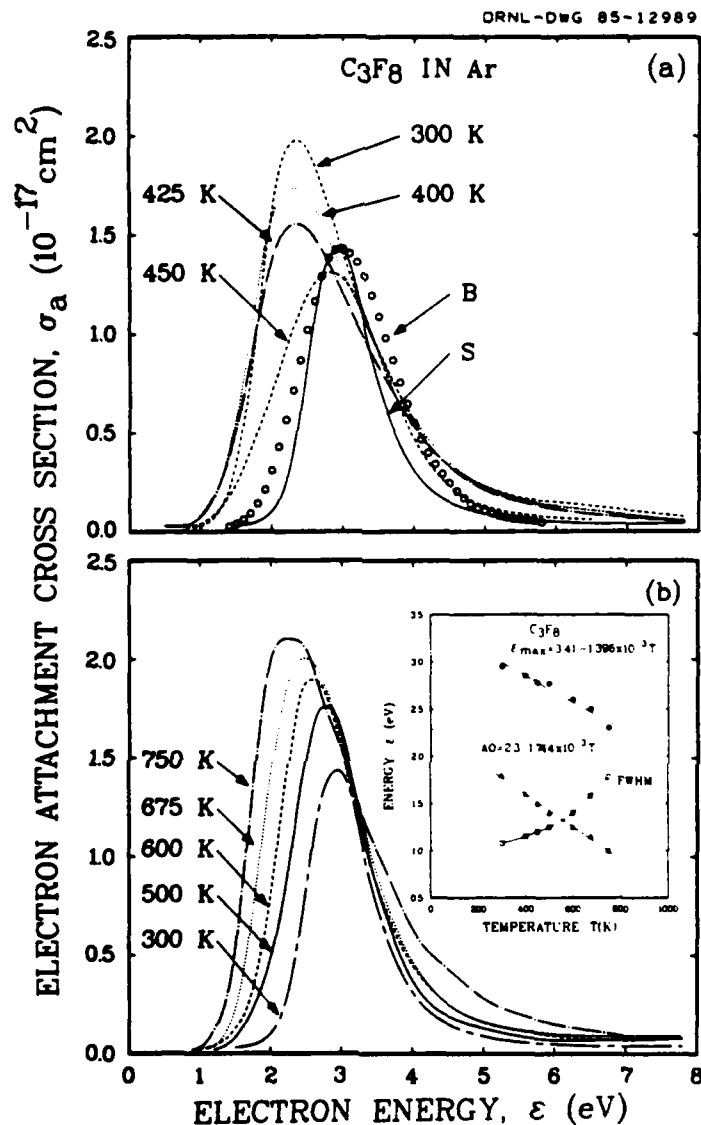


Figure 15. Swarm unfolded total electron attachment cross section $\sigma_a(\epsilon)$ for C_3F_8 obtained [26] from the $k_1(\langle\epsilon\rangle)$ in Ar shown in Fig. 13 at (a) 300, 400, 425, and 450 K and (b) 300, 500, 600, 675, and 750 K. In Fig. 15a is plotted also the dissociative attachment cross section $\sigma_{da}(\epsilon)$ obtained from the swarm data at 300 K (curve S) and the dissociative cross section measured in an electron beam experiment (curve B) which has been normalized to the peak of $\sigma_{da}(\epsilon)$ (see the text). In Fig. 15b the curve for 300 K is the curve S of Fig. 15a. Inset: Variation of peak energy (ϵ_{max}), appearance onset (AO), and full width at half maximum (FWHM) of the total dissociative attachment cross section of C_3F_8 with temperature.

The delicate dependence of $k_a(\langle \epsilon \rangle)$ on T (Figs. 13 and 14) can thus be considered as the result of two opposite effects of T : one on the rate constant for nondissociative and the other on the rate constant for dissociative electron attachment. As it has been shown in the previous section, as a rule, the rate constant for pure nondissociative attachment processes decreases and that for pure dissociative attachment processes increases with increasing T . At each $\langle \epsilon \rangle$, the magnitude of k_a is determined by the relative magnitudes of the rate constants for nondissociative and dissociative electron attachment both of which depend on T . From the data in Fig. 14, it is apparent that for $T \gtrsim 500$ K the principal contribution to the measured k_a originates from dissociative attachment; this is supported by the lack of any dependence of k_a on N_t at high T and from the observed increases in k_a with T^a (500 to 750 K) which are characteristic of molecules^a which attach electrons dissociatively. We then assumed [26] that for $T \gtrsim 500$ K the measured k_a is due entirely to dissociative attachment and extrapolated^a (at various values of $\langle \epsilon \rangle$) the measured k_a at $T \gtrsim 500$ K to lower T (see Figs. 14a,b) in an effort to estimate the dissociative attachment contribution to the measured k_a at $T \lesssim 500$ K, where nondissociative attachment takes place and becomes progressively more significant with decreasing T . From plots such as those in Figs. 14a,b we estimated [26] the ratio $R_{d/t}(\langle \epsilon \rangle)$ of the dissociative to the total attachment rate constant as a function of $\langle \epsilon \rangle$ for 300, 400, 425, and 450 K. These estimates are given in Fig. 14c and show that the contribution of dissociative attachment processes to the measured rate constant is both a function of $\langle \epsilon \rangle$ and T .

The total electron attachment rate constants $k_1(\langle \epsilon \rangle)$ (Fig. 13) were unfolded [26] and the total attachment cross sections $\sigma(\epsilon, T)$ obtained are shown in Fig. 15. They decrease in magnitude with increasing T from 300 to ~ 450 K (Fig. 15a) because in this T range the total cross section contains a large contribution (which decreases as T increases) from nondissociative attachment. An increase in T beyond ~ 450 K (Fig. 15b) results in an overall increase in the magnitude and full width at half maximum--and a shift to lower energy of the onset and energy of the peak (see inset of Fig. 15b)--resulting from the increasingly larger contribution of the dissociative attachment component to the total cross section.

In Fig. 15a are also compared the cross sections due to only the dissociative attachment contribution to the total cross section at 300 K (curve S) and the total (for all fragment anions) dissociative attachment cross section for C_3F_8 measured in a single collision electron beam study [17];

the latter was normalized to the peak value of the former. It is seen that the peak positions of the two cross section functions agree well and that both lie at a higher energy than the total unfolded cross section $\sigma_a(\epsilon, 300 \text{ K})$.

Conclusions

While much improvement in our understanding of the effects of internal energy of a molecule on its electron attaching properties is still desirable, it is clear that as a rule σ_{da} increases and σ_{nd} decreases with increasing T . It is also apparent from the data obtained to date that for both dissociative and nondissociative electron attachment the survival probability is the determining factor (shortening of τ_s in dissociative and shortening of τ_a in nondissociative electron attachment with increasing T) unless geometrical changes concomitant with electron capture effect changes in $\sigma_c(\sigma'_c)$.

From the practical point of view, both the increases and the decreases in $k(\langle\epsilon\rangle)$ with T are significant because they affect the conductivity/dielectric strength properties of the gaseous medium. The sensitivity of $k(\langle\epsilon\rangle)$ to changes in T requires that proper attention be given to the operating temperature range of a given device. Interestingly, the sensitivity of $k(\langle\epsilon\rangle)$ to T (e.g., C_6F_6 ; see Fig. 12) can perhaps be employed to change the conducting/insulating properties of a gaseous medium by varying T .

Acknowledgments

Research sponsored in part by the Office of Health and Environmental Research, U.S. Department of Energy, under contract DE-AC05-84OR21400 and in part by the Office of Naval Research under interagency agreement 43 01 24 60 2 with Martin Marietta Energy Systems, Inc.

References

- [1] Christophorou, L. G. *Environ. Health Perspect.* 1980, 36, 3.
- [2] Christophorou, L. G.; McCorkle, D. L.; Christodoulides, A. A. In "Electron-Molecule Interactions and Their Applications"; Christophorou, L. G., Ed.; Academic Press: New York, 1984; Volume 1, Chapter 6.

- [3] O'Malley, T. F. Phys. Rev. 1966, 150, 14.
- [4] Bardsley, J. N.; Herzenberg, A.; Mandl, F. Proc. Phys. Soc. (London) 1966, 89, 321.
- [5] O'Malley, T. F. Phys. Rev. 1967, 155, 59.
- [6] Christophorou, L. G. "Atomic and Molecular Radiation Physics"; Wiley-Interscience: New York, 1971; Chapter 6.
- [7] Chantry, P. J. J. Chem. Phys. 1969, 51, 3369.
- [8] Bardsley, J. N.; Wadehra, J. M. Phys. Rev. 1979, 20, 1398.
- [9] Bardsley, J. N.; Wadehra, J. M. J. Chem. Phys. 1983, 78, 7227.
- [10] Christophorou, L. G. J. Chem. Phys. (submitted).
- [11] Allan, M.; Wong, S. F. J. Chem. Phys. 1981, 74, 1687.
- [12] Christophorou, L. G.; Compton, R. N.; Dickson, H. W. J. Chem. Phys. 1968, 48, 1949.
- [13] Huber, K. P.; Herzberg, G. "Molecular Spectra and Molecular Structure. IV. Constants of Diatomic Molecules", Van Nostrand Reinhold Company: New York, 1979.
- [14] Allan, M.; Wong, S. F. Phys. Rev. Lett. 1978, 41, 1791.
- [15] Spyrou, S. M.; Christophorou, L. G. J. Chem. Phys. 1985, 82, 2620.
- [16] Christophorou, L. G.; McCorkle, D. L.; Anderson, V. E. J. Phys. B 1971, 4, 1163.
- [17] Spyrou, S. M.; Sauers, I.; Christophorou, L. G. J. Chem. Phys. 1983, 78, 7200.
- [18] For O_2 we used the calculated values of O'Malley [5] which fitted well the experimental results.
- [19] These cross sections were obtained using the relative cross section data of Ref. 11 at various T and by normalizing these to the room temperature cross section values of Ref. 12.
- [20] These cross sections were obtained using the relative cross section data of Ref. 7 at various T and normalizing the room temperature intensity at 2.3 eV to $8.3 \times 10^{-18} \text{ cm}^2$ [21].
- [21] Chaney, E. L.; Christophorou, L. G. J. Chem. Phys. 1969, 51, 883.
- [22] Chen, C. L.; Chantry, P. J. J. Chem. Phys. 1979, 71, 3897.
- [23] The cross sections at various T were obtained using the relative cross section of Ref. 22 and taking for the cross section maximum for SF_5/SF_6 at 0.37 eV [24] the value [25] of $9.8 \times 10^{-16} \text{ cm}^2$. Since in the time-of-flight studies of Ref. 24 the temperature was higher ($\sim 350 \text{ K}$) than ambient (due to heating of the collision chamber by the filament), it was assumed that the $9.8 \times 10^{-16} \text{ cm}^2$ value corresponds to $T \approx 355 \text{ K}$.

- [24] Christophorou, L. G.; McCorkle, D. L.; Carter, J. G. J. Chem. Phys. 1971, 54, 253.
- [25] Christophorou, L. G.; McCorkle, D. L.; Carter, J. G. J. Chem. Phys. 1972, 57, 2228.
- [26] Spyrou, S. M.; Christophorou, L. G. J. Chem. Phys. (in press).
- [27] Spence, D; Schulz, G. J. J. Chem. Phys. 1973, 58, 1800.
- [28] Shimanouchi, T. NSRDS-NBS 39, June 1972.
- [29] N₂O has three normal modes: NN stretch (2224 cm⁻¹), bend (589 cm⁻¹), and NO stretch (1285 cm⁻¹) [28].
- [30] Hickam, W. M.; Berg, D. J. Chem. Phys. 1958, 29, 517.
- [31] Hunter, S. R.; Christophorou, L. G.; McCorkle, D. L.; Sauers, I; Ellis, H. W.; James, D. R. J. Phys. D 1980, 16, 573.
- [32] McCorkle, D. L.; Christophorou, L. G.; Hunter, S. R. In "Proceedings of the Third International Swarm Seminar"; Lindinger, W.; Villinger, H.; Federer, W., Eds.; Innsbruck, Austria, 1983; p. 37.
- [33] Spyrou, S. M.; Christophorou, L. G. J. Chem. Phys. 1985, 82, 1048.
- [34] Hunter, S. R.; Christophorou, L. G. J. Chem. Phys. 1984, 80, 6150.

END

FILMED

12-85

DTIC